NWC TP 5497

Progress Report on Electrical Resistivity Studies, Coso Geothermal Area, Inyo County, California

by

Robert B. Furgerson
Colorado School of Mines
for the
Propulsion Development Department

Naval Weapons Center
CHINA LAKE, CALIFORNIA ■JUNE 1973

ABSTRACT

This report describes the first phase of an electrical geophysical survey being conducted in the vicinity of the Coso Hot Springs, California, and contains data obtained through June 1972. The Coso Geothermal Area has been selected as an area for investigation and evaluation of its potential for geothermal energy.

NWC Technical Publication 5497

Published by . . . . . Propulsion Development Department
Collation . . . . . Cover, 34 leaves, DD Form 1473, abstract cards
First printing . . . . . 365 unnumbered copies
Security classification . . . . . UNCLASSIFIED

Naval Weapons Center

AN ACTIVITY OF THE NAVAL MATERIAL COMMAND

Paul E. Pugh, RADM, USN ..... Commander

Walter B. LaBerge, Ph.D. ..... Technical Director

FOREWORD

This report is part of a continuing investigation of the geology of the Naval Weapons Center's test range areas.

Released by
G. W. Leonard, *Head,*
Propulsion Development Department

Under Authority of
WALTER B. LaBERGE
Technical Director

CONTENTS

ACKNOWLEDGEMENTS

It is necessary to thank many people without whom this investigation would not have proceeded to its present stage. Mr. Kenneth Pringle and Mr. Kenneth Rinehart, Naval Weapons Center personnel, assisted in the field work. The University of California, Riverside (where the author was attending graduate school at the time), Dr. George V. Keller of Group Seven, Inc., and the Naval Weapons Center provided instrumentation. My wife, Deborah Rae, deserves enormous thanks for illustrating the many figures.

INTRODUCTION

The Coso Geothermal Area is located primarily within the Naval Weapons Center (NWC) test ranges north of China Lake in Inyo County, California. This area is about 125 miles north-northeast of Los Angeles and is just east of the Sierra Nevada Mountains. Figure 1 is an index map showing the general location of the geothermal area. The prospect area is covered by four U. S. Geological Survey topographic maps at a scale of 1:62,500; these are the Haiwee Reservoir, Coso Peak, Little Lake, and Mountain Springs Canyon quadrangles. Elevations in the surveyed area range from about 3300 ft above sea level in Rose Valley to about 5500 ft in the Coso Range.

FIG. 1. Index Map for the Coso Geothermal Area, Inyo County, California.

This report describes work conducted during the first phase of an electrical geophysical survey of the Coso Geothermal Area. The objective of the survey was to outline areas of anomalously conductive ground which may be associated with geothermal activity and to assist in locating drilling sites to test the geothermal potential.

GENERAL GEOLOGY AND STRUCTURE

The general geology of the Coso Geothermal Area has been described by Fraser and others (Ref. 1), Ross and Yates (Ref. 2), Chesterman (Ref. 3), Austin (Ref. 4), and Koenig and others (Ref. 5). Some of these authors also compiled geologic maps at various scales as did Jennings (Ref. 6), Moyle (Ref. 7), and M. Stinson (unpublished mapping, Calif. Division of Mines and Geology). According to Fraser and others (Ref. 1),

> "The central part of Coso Mountains is composed of very coarse-grained granitic rock. Areas of diorite, horneblende gabbro, and other basic rocks occur in the granite, some as gneissic or schistose zenoliths, and others as elongated dike-like masses which apparently intruded the granite. Lying upon the deeply weathered and eroded surface of the granite basement are a number of alluvial fans, best seen along the western flank of the range but also present along the northern and northeastern borders. The southern part is covered in many places by extensive but relatively thin beds of well-stratified tuff and volcanic breccia. The tuff, breccia, and alluvium all dip away from the crest of the range at low angles ranging between 6 and 10 degrees. Above the tuffs and conformable with them is a basaltic lava 50 to 100 feet thick. Associated with this lava in places are partially preserved basaltic cinder cones. Subsequently there were extensive flows of rhyolitic [and/or andesitic] material; well-formed rhyolitic cinder cones may be seen along a north-south line about 3 miles west of Coso Hot Springs. In places these late rhyolite flows are covered with a shallow mantle of ash and volcanic tuff, some of which is unconsolidated, but in other places it is cemented by fine-grained silica....On the basis of some vertebrate fossils found in the sediments underlying the older tuff beds, Schultz (Ref. 8) dated these sediments as transitional between lower and upper Pliocene. Consequently all of the volcanic activity is later than upper Pliocene and some undoubtedly belongs in the late Pleistocene or Recent."

According to Ref. 4, 5, and 9, the Coso Geothermal Area is located within the junction of two major structure trends. One of these is the essentially north-south fault system that borders the eastern scarp of the Sierra Nevada. The second of these is a major northwest-trending tear fault system with movement considered to be left lateral. The Wilson Canyon Fault Zone is a member of this system as is its western extension which can be traced from east of the Argus Range well into the Sierra (Ref. 7 and 9). Figure 2 shows it has a trend of N60°W where it crosses T.23S., R.38 and 39E. Another member of the system is the Darwin Tear Fault located some 20 miles to the northeast (Hall and

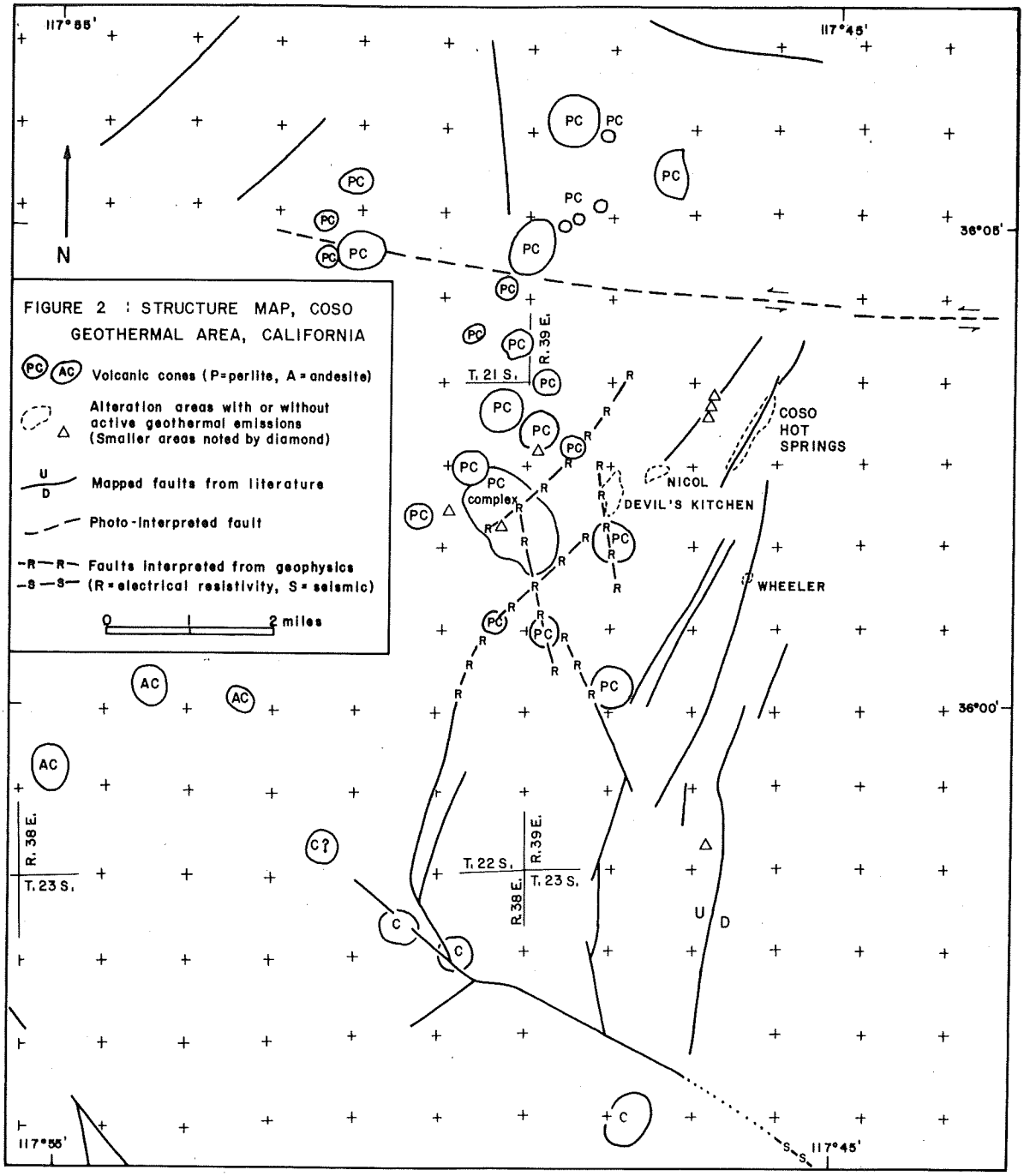

FIGURE 2 : STRUCTURE MAP, COSO GEOTHERMAL AREA, CALIFORNIA

PC AC Volcanic cones (P=perlite, A=andesite)

Alteration areas with or without active geothermal emissions (Smaller areas noted by diamond)

U/D Mapped faults from literature

Photo-interpreted fault

-R—R- Faults interpreted from geophysics

-S—S- (R=electrical resistivity, S=seismic)

MacKevett, Ref. 10). Both of these fracture systems appear to offset the eastern face of the Sierra.

Within this structural junction is the Coso Geothermal Area, and Austin and others (Ref. 9) have used photo-interpretation of photo-mosaics to show that the area is characteristic of a caldera--mild doming and fracturing followed by vulcanism and surficial subsidence. The vulcanism which consisted of a mixture of explosion breccia rings, extrusive perlite domes, and obsidian sills (Ref. 5) occurred along radial trending fractures within the subsidence zone and along marginal arcuate (or cylindrical) fractures in the surrounding granitics and overlying basalt flows (Fig. 3). According to Ref. 9 (p. 10 and Fig. 9),

> "....the controlling or primary magmatic chamber patterns range from 25 to 30 miles in length and 15 to 20 miles in width. Within the controlling primary pattern are smaller patterns generally 4 to 6 miles in diameter. These smaller circular to elliptic patterns are believed to represent the surface expression of underlying stocks and apophyses of stocks and to mark the active geothermal cells suitable for exploration."

According to Ref. 1, most of the rhyolitic flows, obsidian, tuff, and volcanic breccia which occur throughout the Coso Geothermal Area apparently are derived from a nearly north-south line of craters located one-half mile west of Devil's Kitchen. Some of these cones are more than 700 feet high, nearly circular, and composed of glassy lava fragments showing good flow structure. The large quantity of volcanic ash and breccia which blankets the surrounding country attests to the explosive character of at least some of the eruptions. Ross and Yates (Ref. 2) note that many of the younger cones are breached on the south and southwest sides and so make the interesting speculation that the conduits may plunge to the north or northeast.

The latest stage of the volcanic activity is represented by presently active hot springs and fumeroles. Active leaching and alteration of the wall rocks is in progress and native sulphur, iron and aluminum sulphates, and possibly cinnabar are still being deposited. The area presents an interesting example of intense solfataric alteration in siliceous rocks. The most conspicuous of these areas of surface geothermal emissions are named Devil's Kitchen, Nicol prospect, Coso Hot Springs, and Wheeler prospect. The position of these and other minor areas is shown in Fig. 2. The Coso Hot Springs are very clearly arranged along the east side of a small fault scarp which trends N30°E and dips presumably to the east (Ref. 1). This fault parallels the trend of the valley and is probably subsidiary to a major fault system. In the vicinity of the hot springs, the fault shows a well-defined scarp that has an average elevation of about 5 to 10 ft (Fig. 4). This fault can be traced for at least a mile and one-half to the northeast. A short distance south of the Coso Road it disappears in the granite.

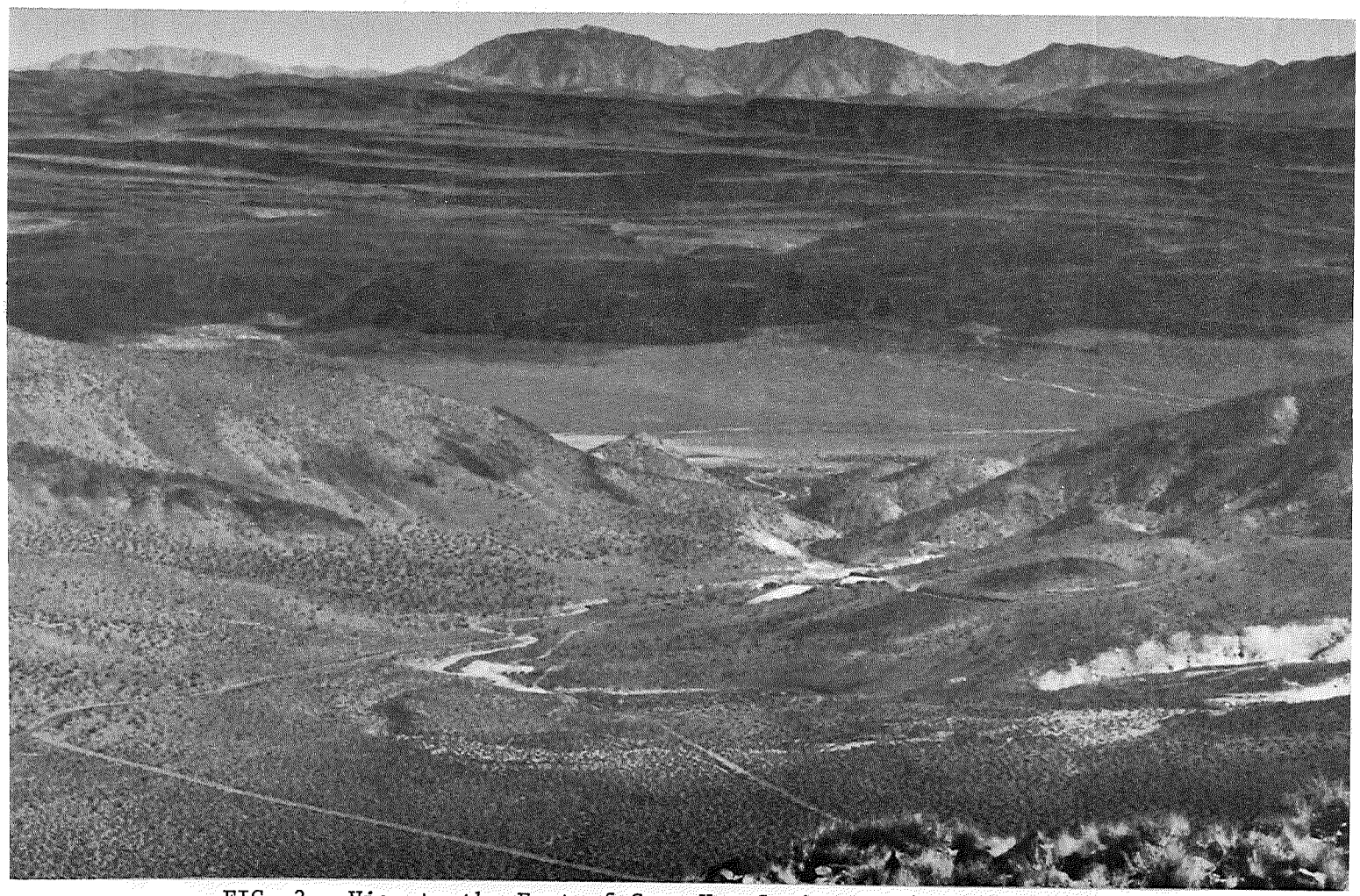

FIG. 3. View to the East of Coso Hot Springs. The mountains in the background are cut by a complex series of step faults, and basalt flows cover a large portion of these mountains.

NWC TP 5497

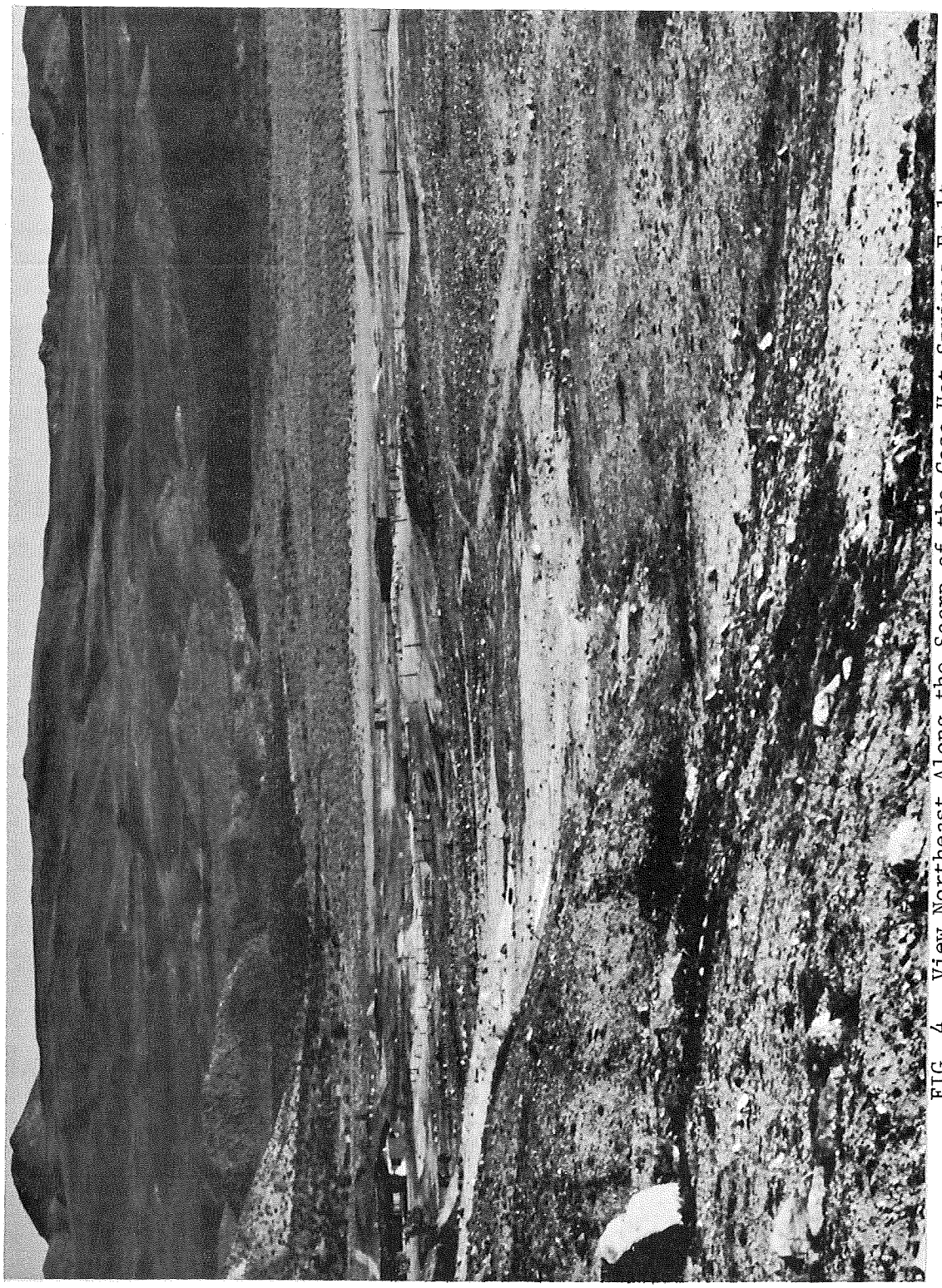

FIG. 4. View Northeast Along the Scarp of the Coso Hot Springs Fault along which is a Zone of Active Hot Springs and Fumeroles.

Fraser and others (Ref. 1) feel that the presence of elements such as manganese, boron, zinc, lead, tin, vanadium, titanium, nickel, chromium, bismuth, and silver in the analysis of water samples from the springs is strongly suggestive of a hypogene origin. However, Frazer notes that most of the springs show a marked seasonal variation in flow and so concludes that there is considerable intermixing of ground water and meteoric waters in these springs. Another, in fact more important, problem in making geochemical analyses is the large amount of chemical contamination in the area. According to Austin and Pringle (Ref. 11), the contaminants are galvanized iron (pipes, tubs, and siding) that provides abundant iron and zinc; brass valves and the residue from the U. S. Bureau of Mines copper plate experiments (Dupuy, Ref. 12) that provide copper; tin cans that provide tin, lead, and iron; coins that provide nickel, silver, and copper; and scrap wood, dead animals (numerous cattle), and animal effluvia that provide nitrate and ammonia.

PLAN OF THE ELECTRICAL SURVEY

The electrical resistivity of a rock is a measure of the resistance to the flow of electrical current and is determined almost entirely by the amount and resistivity of the water contained in its pores. The water resistivity depends on the nature of the dissolved salts and on temperature. It is this dependence on temperature that makes electrical resistivity measurements such a useful technique in investigating geothermal systems. With an increase in temperature and in the amount of dissolved salts, the resistivity of a rock will decrease until the boiling point is reached, past which the resistivity rapidly increases. The ratio of the resistivity of the host rock to that in the geothermal cell is defined as the Geothermal Resistivity Index (GRI). If the salinity of the pore water is the same in the geothermal reservoir and and in the host rock, then the GRI is a very good indication of the elevation of temperature inside the cell and must be at least 5 if the reservoir is to produce power (George Keller, personal communication).

Banwell (Ref. 13) recommends that the geophysical procedure to be used in delineating a geothermal reservoir should be profiling with the direct-current resistivity method, combined with direct-current resistivity soundings to depths of the order of 2 miles. Schlumberger profiling, as recommended by Banwell, is difficult to use in mountainous terrain such as that of the Coso area and can provide ambiguous results if there are rapid lateral changes in resistivity, as are frequently associated with geothermal systems. Therefore, no profiling was attempted in this survey and direct-current resistivity sounding was started with the Schlumberger array. After 12 soundings it was decided to switch the bulk of the effort to a dipole mapping survey as described by Furgerson (Ref. 14) under the name "controlled-source telluric current technique". This was because the soundings were going too slow (an

average of one day per 3000 ft AB/2 sounding) to cover the prospect area in a reasonable time.

In a dipole mapping survey, electric field measurements are made at distances up to 4 miles or more from a dipole source of current, providing information on an average resistivity to a comparable depth. Therefore, dipole mapping surveys are useful in mapping the geographical extent of deep-lying geothermal reservoirs, but provide relatively little information on the variation of resistivity with depth in the ground. Once the extent of a reservoir has been determined, other means must be used to determine the depth to the top and bottom of the reservoir. Such information can be obtained with more Schlumberger soundings and the electromagnetic sounding method after dipole mapping is completed.

SCHLUMBERGER SOUNDING

An electrical resistivity sounding consists of a succession of apparent resistivity measurements made with an increasing electrode separation, the center of the configuration and its orientation remaining constant. With larger electrode separations, the effect of material at depth becomes more pronounced, and thus the apparent resistivity values made at the ground surface reflect the vertical distribution of resistivity values in a geological section. There are rather severe limits on the amount of lateral variation in resistivity permitted with this method.

The Schlumberger electrode configuration (Chastenet de Gery and Kunetz, Ref. 15, and Keller and Frischknecht, Ref. 16) consists of two current electrodes, A and B, and two potential electrodes, M and N, spaced along a straight line as shown in Fig. 5. The potential electrodes are placed an equal distance about the midpoint between the

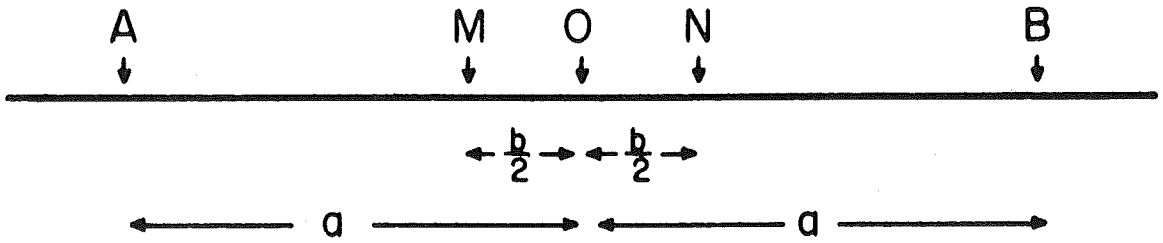

FIG. 5. Schlumberger Electrode Array Geometry.

current electrodes and are kept sufficiently close together so that the electric field between them can be considered constant. In practice, the separation of potential electrodes M and N is always kept less than one-fifth of the separation between the current electrodes A and B. The formula used for the apparent resistivity is

$$\rho_a = K \frac{\Delta V}{I}$$

where ΔV is the potential difference between the potential electrodes, I is the current input to the ground between the current electrodes, and K is the geometric factor which takes the exact location of all four of the electrodes into account

$$K = \frac{2\pi}{\frac{1}{AM} - \frac{1}{AN} - \frac{1}{BM} + \frac{1}{BN}}$$

With the symmetry described above and letting AB/2 = a and MN = b

$$K = \pi\left(\frac{a^2}{b} - \frac{b}{4}\right)$$

Only one set of electrodes, either the current or the potential, is moved between successive measurements. Thus the potential electrodes remain fixed for several (usually 3 to 5) increasingly expanded current electrode spacings. Measurements were made with "a" spacings of 20 ft minimum to 3000 ft maximum--the maximum spacing depending on terrain and the signal-to-noise level. The measurements were made to give about 7 points per decade on a logarithmic plot of AB/2 versus apparent resistivity (see Appendix A).

The transmitter system consisted of a 3.0 kw, 115 vac, 60 Hz, portable generator and a Geoscience Corp. 4.0 kw rectifier-switch (5.0 amp maximum, 800 volt maximum). The output wave form is a square wave, and the frequency and wave symmetry are variable. The frequencies used in the survey varied between 1.0 and 0.05 Hz and generally were selected by consideration of the skin depth, the depth at which the amplitude of an electromagnetic wave is reduced to $1/e$ of its surface value. If the magnetic permeability is taken to be that of free space (a valid assumption for the majority of earth materials), Stacy (Ref. 17) gives the skin depth for a homogeneous half space as

$$z = (2\pi\ \omega\ \sigma)^{-\frac{1}{2}}$$

where

z = skin depth in cm

ω = angular frequency = $2\pi f$

σ = electrical conductivity in mhos = 1 / electrical resistivity in $(\text{ohm-m})^{-1}$

When the frequency is too high for the depth resistivity combination, the apparent resistivity obtained will be too high. A simple empirical test (Meidav and Furgerson, Ref. 18) was used to determine the reliability of a measurement. Readings were taken at more than one frequency at a given electrode spacing. Hence, a difference in potential electrode voltage of more than 3 to 5% between two frequencies was used to judge the quality of the data. The data obtained with longer periods were deemed more reliable. Coupling between current and potential lines occasionally caused an erroneous increase in the apparent resistivity and was corrected by separating the current and potential wires by 5 to 20 ft.

The receiver consisted of an Esterline Angus model T-100 battery-operated chart recorder with a maximum sensitivity of 2 millivolts full scale. An auxiliary zero adjustment was needed when excessive electrode potentials and/or self potentials were encountered. Figure 6 shows the transmitter and receiver set up in the back of a vehicle for operation.

Interpretation was started by decomposing (or inverting) the field curves into layer thicknesses and layer resistivities, assuming a horizontally-layered structure. How "true" the values of thickness and resistivity are depends on the degree of validity of assuming a horizontally-layered structure; how equivalent the curve is; the available correlations; and the technique used in accomplishing the actual inversion.

Several methods can be used in attempting to determine whether a field curve is the result of horizontal layering. One of the best is to make soundings at the same location but with different azimuths; these curves should be the same if the structure is indeed horizontally-layered. Another is to make two other potential measurements in addition to V_{MN}; these are V_{MO} and V_{ON} (Fig. 5). For a horizontally-layered structure or for a sounding made parallel to the strike of a dipping layered structure, V_{MN}, V_{MO}, and V_{ON} should be equal. For a sounding made at some other angle to the strike of a dipping structure, $V_{MO} < V_{MN} < V_{ON}$ or $V_{MO} > V_{MN} > V_{ON}$. Because of the large amount of area to be covered, the first method could not be employed, and because of the low sensitivity of the receiver used and the high contact resistance, low signal-to-noise levels prevented the use of the second method. Therefore, a horizontally-layered structure was assumed in the first stage of interpretation for lack of conflicting evidence.

When different sets of layering parameters provide the same theoretical sounding curve within some small error (usually taken as 5%), these sets of conditions are said to be equivalent. Thus there exists a strong probability that the interpretation of a field curve will not be unique unless some means of correlation is possible.

FIG. 6. Typical Set-Up for Schlumberger Electrical Resistivity Sounding.

Electrical logs are ideal for such correlation, but unfortunately none are available in the area; in fact there are only two wells deeper than 100 ft (Fig. 7). One is a water well at Coso Junction, but no stratigraphy and only a very questionable water depth of 250 ft is available. The other is the Coso No. 1 with a total depth of 375 ft (Ref. 11).

Some gravity and seismic data are also available on Rose Valley (Healy and Press, Ref. 19, Fig. 3, 8, and 9; on their Fig. 9, the latitude values should read 35° 50' and 36° 00' instead of 36° 00' and 36° 10') which can be used to help interpret sounding HR-9 of Appendix A. Using a density contrast of 0.5 g/cc, they obtained a computed depth to basement of 5600 ft for a northeast-southwest gravity profile one-half mile south of HR-9. Two attempts were made to obtain good basement arrivals on seismic refraction profiles expanded northwest-southeast along the power line road one-quarter mile northeast of HR-9. A weak arrival with apparent velocity of 15,000 ft/sec indicated a depth of about 2100 ft, but this depth does not agree with their gravity interpretation. Healy and Press feel that the most likely explanation for this disagreement is that the weak, high velocity arrival comes from an inter-bedded volcanic layer.

Interpretation of each sounding consisted of three steps. The first involved making a graphical interpretation by the auxiliary point method (Zohdy, Ref. 20, and Orellana and Mooney, Ref. 21). Quite often the auxiliary point interpretation made in the field was close enough and another did not have to be made. In the second step the auxiliary interpretation and the field curve were input into a computer program developed by Crous (Ref. 22) which Hankel-transforms the field data into the ''kernal'' domain and, with the auxiliary curve interpretation as a first cut, arrives at an interpretation by a least squares fitting routine. The output is in terms of each layer's longitudinal conductance (S) or transverse resistance (T). In the third step, the values of S and T were converted to layer thicknesses and resistivities. These values were then input into a computer program which computes theoretical sounding curves for the Schlumberger array over a multi-layered horizontal earth. This computer program was produced by the Geophysical Institute of Israel using a Fortran conversion of an Algol program by Argelo (Ref. 23). The interpretation was modified, when necessary, to obtain a better fit between the field data and the computer-generated model.

Locations of the 12 soundings taken so far in the survey are shown in Fig. 7. The field data and the interpretations obtained by the procedure described above are given in Appendix A. A discussion of these interpretations in conjunction with the dipole mapping survey is contained in the section EVALUATION OF SURVEY DATA.

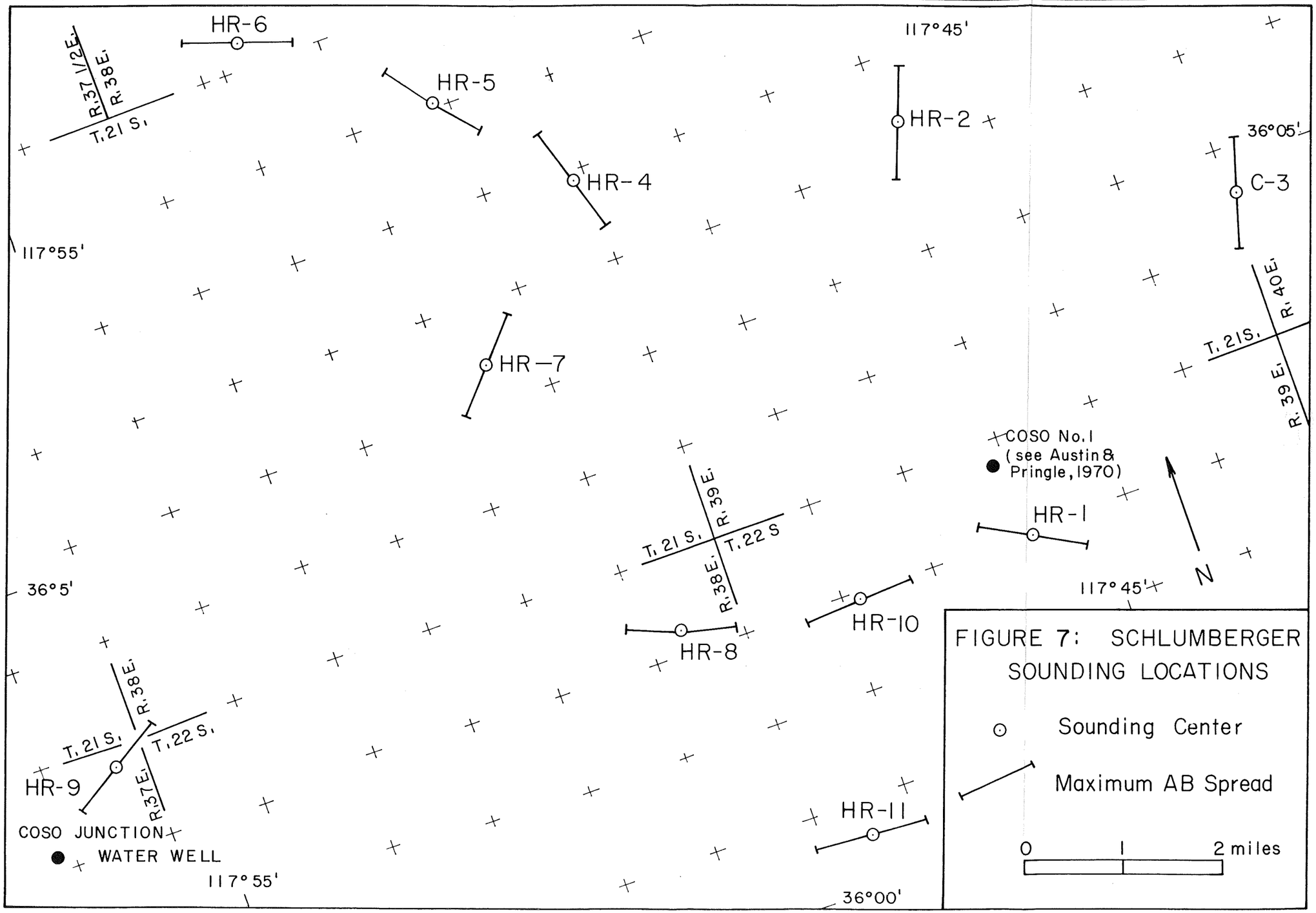

FIGURE 7: SCHLUMBERGER SOUNDING LOCATIONS

⊙ Sounding Center

Maximum AB Spread

DIPOLE MAPPING SURVEY

In a dipole mapping survey (Ref. 14), a large amount of electric current is caused to flow in the earth between electrode contacts situated a mile or more from the target area. As the current flows through the ground from this "dipole" source, its flow pattern will be governed by variations in resistivity in the ground to a depth comparable to the offset distance at which the measurements are being made. Because the dipole source is fixed in location while many measurements of electric field are made about it, any electrical non-uniformities near the source will affect all the measurements similarly, and the variation in the characteristics of the electric field from observation point to observation point will be indicative of the electrical structure of the ground primarily in the vicinity of the measurement points.

The general scheme of a dipole mapping survey is indicated in Fig. 8. A and B are current electrodes, $\overline{MN}_1$ and $\overline{MN}_2$ are voltage measuring dipoles, δ is the angle between the measuring point and the source electrodes, Θ is the angle between the voltage measuring dipoles, and R_1 and R_2 are the distances from the measuring point to the source electrodes. This array

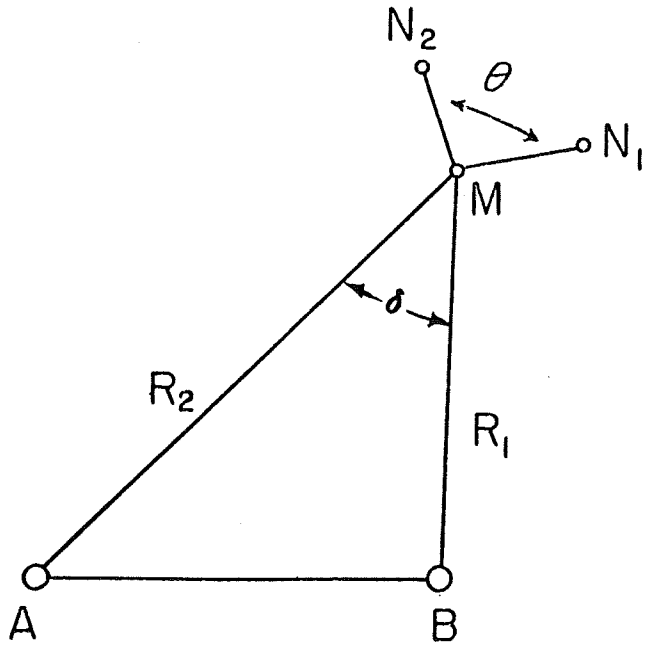

FIG. 8. General Scheme of a Dipole Mapping Survey.

is superficially similar to an azimuthal dipole-dipole array. However, for the electrode separations $\overline{AB}$ and $\overline{MN}$ to approximate true dipoles, the separation between them should be at least five times greater than the larger of $\overline{AB}$ or $\overline{MN}$ (Alpin, Ref. 24). Experience, however, shows that for

a large $\overline{AB}$, practical current moments of 20,000 to 200,000 amp-m give reliable field strengths for distances up to five or at the most ten times $\overline{AB}$. The parameter "current moment" is defined as the product of the current flowing into the ground through the current electrodes times the distance between the current electrodes. For a given resistivity distribution in the ground, the field strength at a particular observation point is proportional to the current moment. Thus most of the stations must be located at distances R_1 for which the array is more properly termed a quadripole array for a very small R_1 or a pole-bipole array for a larger R_1.

Source dipoles of 1.1 and 1.3 miles length were used in this survey, and the source electrodes were grounded through 8 to 12 ft lengths of aluminum rod, with the ground soaked with salt water to insure good grounding. The holes for one source dipole were drilled with a portable motor-driven auger, but this technique required considerable time because of large cobbles and caliche layers. The holes for the second source dipole were made with the shaped charge explosives from Zuni M-5 rockets (Fig. 9).

Power was provided to the source dipole from a 10 kw motor-generator set. The 220 volt 60 Hz single-phase output of the generator was stepped up to 440 volts with a transformer, rectified to form direct current, and alternately switched to cause current to flow first one way and then the other in the line connecting the source electrodes. The period between one complete cycle of current flow was selected to be 20 seconds, so that the frequencies contained in the waveform of the current would be sufficiently low to avoid problems with electromagnetic attenuation of the current field and lack of penetration caused by skin-depth effects. The current waveform was asymmetrical to provide a means for assigning a polarity to voltage detected at the receiving sites. The amplitude of the current steps was recorded graphically, and current steps with amplitudes of 1 to 10 amperes were used. Figure 10 shows the transmitting instrumentation set up at Source 2.

The electric field from a source dipole was mapped by measuring voltages between electrode pairs at many points about the source dipole. Because the direction of current flow at a measurement site is quite unpredictable, the total voltage drop must be determined by making measurements with two electrode pairs oriented at close to right angles to one another and adding voltages vectorially. The electric field is then assumed to be the ratio of voltage drop to the separation between the measuring electrodes. Measurements were made with receiving electrode separations of 100 to 300 ft, the longer separation being used in areas where the signal strength was low. The receiver was a sensitive DC voltmeter and consisted of a high-gain, low-noise, operational amplifier with high input impedence (1×10^6 ohms), coarse and fine DC offsets, and a maximum sensitivity of 20 microvolts per dial division. An output jack enabled chart recording of the data when desired.

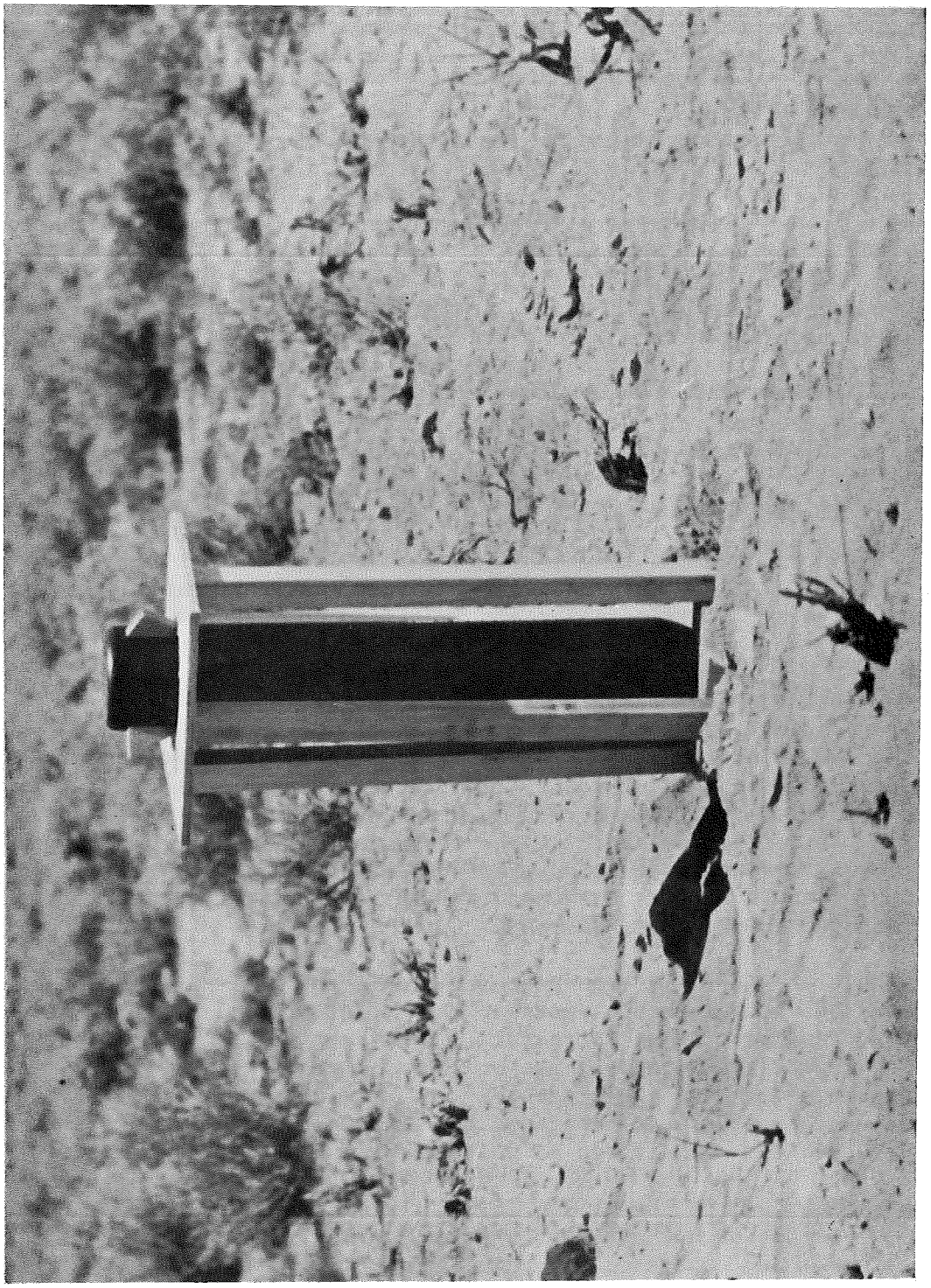

FIG. 9. Shaped-Charge Explosive From a Zuni M-5 Rocket Used to form Electrode Holes for Source 2.

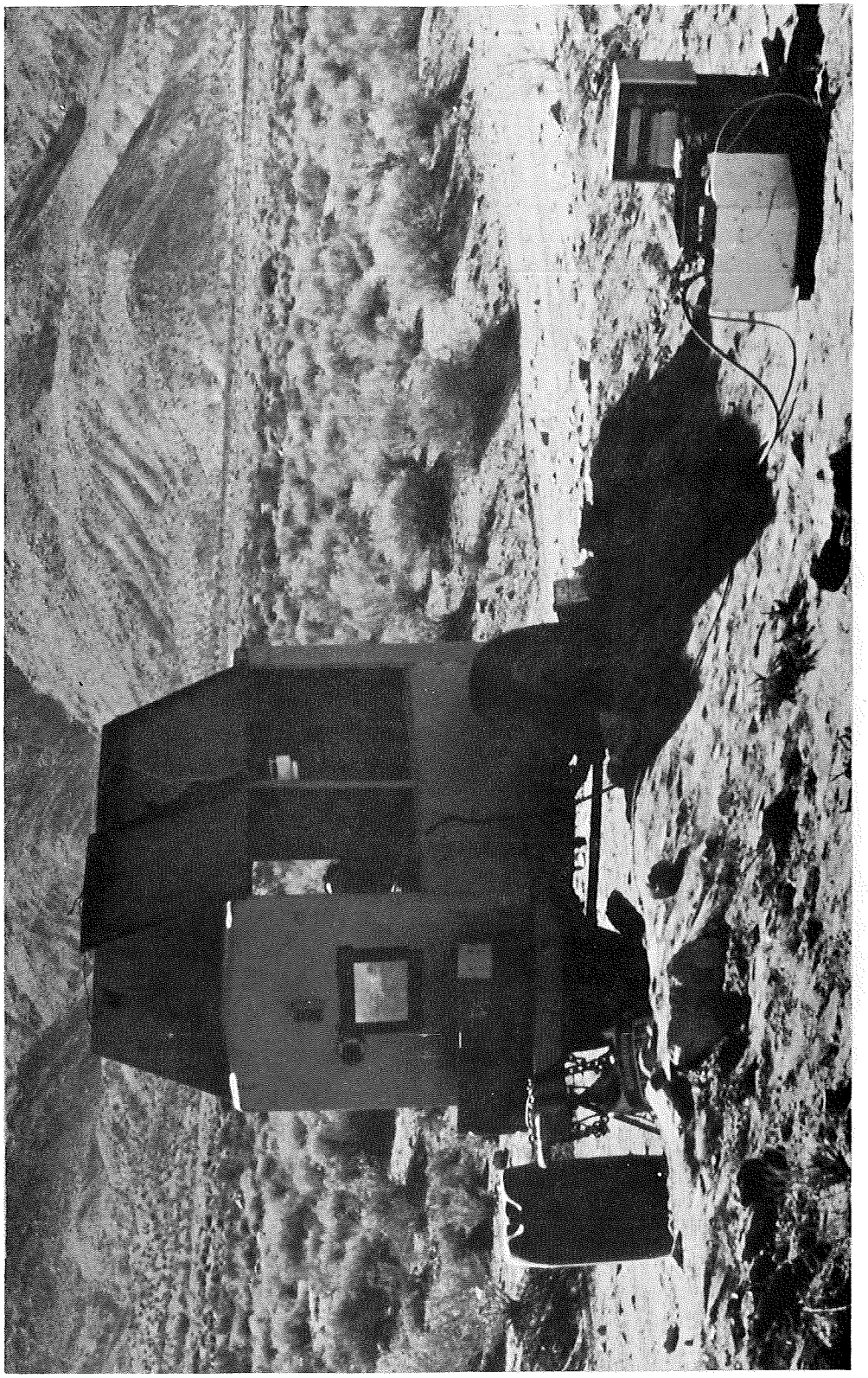

FIG. 10a. General View of the Generator and transmitter Set-Up at Source 2.

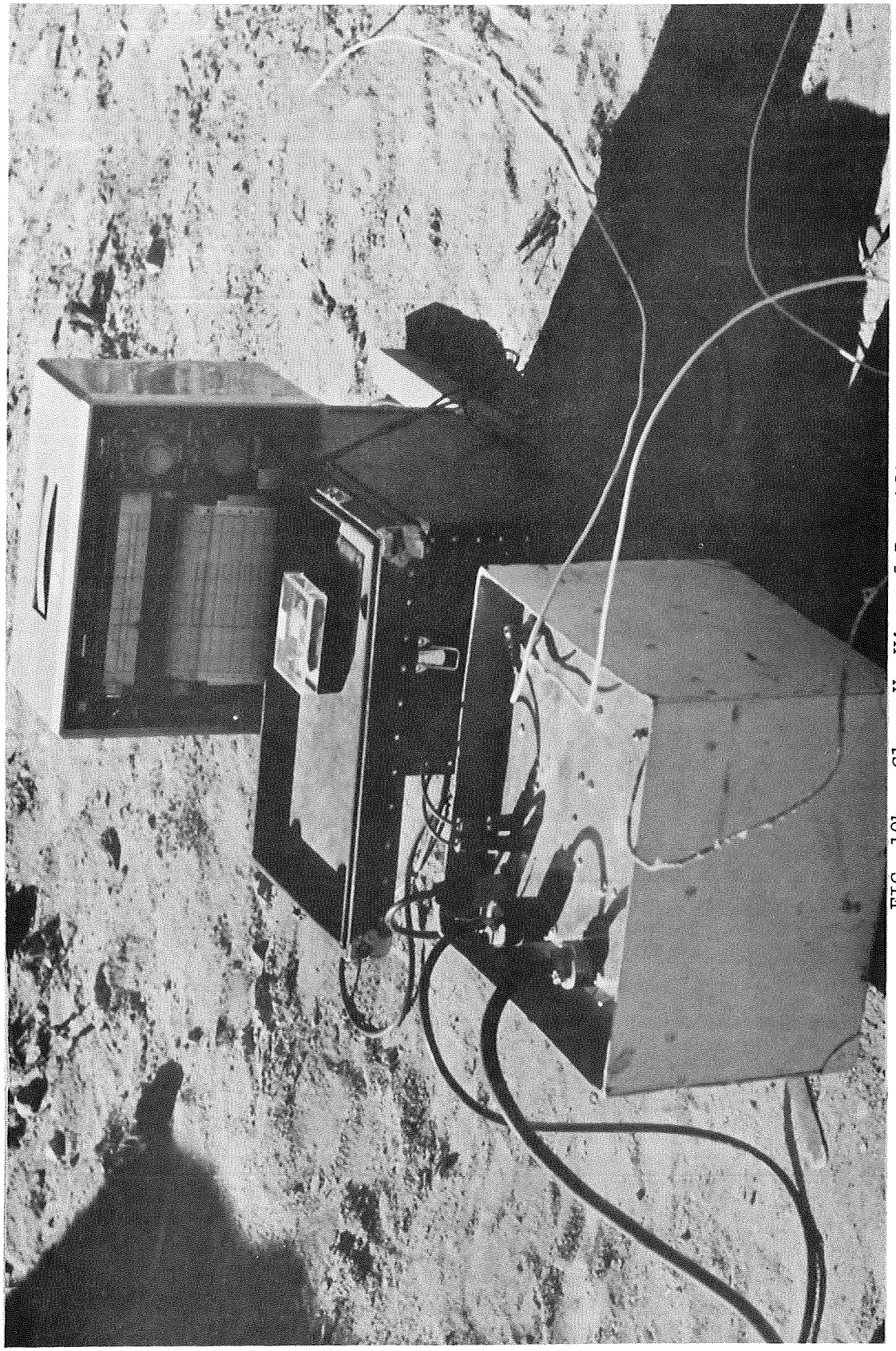

FIG. 10b. Close-Up View of Rectifier-Switch and Output-Current Recorder.

Electric fields were measured at distances from a source dipole ranging up to 4 miles. Measurements were usually not made closer than about one-half mile from the end of a source dipole, because an advantage in using the dipole mapping technique lies in the capacity to make measurements at sufficient distance to assure penetration to depths of many thousands of feet. Measurements made close to one end of a dipole source will reflect the resistivity only to a shallow depth, comparable to the distance from the end of the line. Several dipole sources are being used to provide adequate coverage and to insure a reasonable amount of overlap so that areas which appear to be promising will be covered with measurements made from more than one source. So far about 200 measurements have been made around two sources (see Fig. 11 and 12 for location maps), and the primary data obtained are listed in Appendix B. These data may be converted to apparent resistivity values using several different formulas.

The conventional manner of defining apparent resistivity is to consider what resistivity a uniform earth would require to provide the voltages actually measured. In a uniform earth, current spreads out from a single electrode with spherical symmetry. The electric field strength on the surface of the earth at a distance R_1 from a single electrode through which a current I is passing is then

$$E_1 = \frac{\rho I}{2\pi R_1^2}$$

where ρ is the resistivity of the assumed uniform earth. When a dipole pair of electrodes is used for a current source, there is a second contribution to the electric field from the current flowing through the second electrode:

$$E_2 = \frac{\rho I}{2\pi R_2^2}$$

where R_2 is the distance from the observation point to the second current electrode. The electric fields E_1 and E_2 are vector quantities, and must be added vectorially. The vector sum is

$$E_T = \frac{\rho I}{2\pi R_1^2}\left[1 + \left(\frac{R_1}{R_2}\right)^4 - 2\left(\frac{R_1}{R_2}\right)^2 \cos\delta\right]^{1/2}$$

Solving this expression for ρ provides the means for computing apparent resistivity under the assumption of spherically-symmetric spreading of current in a uniform earth. Values for apparent resistivity computed

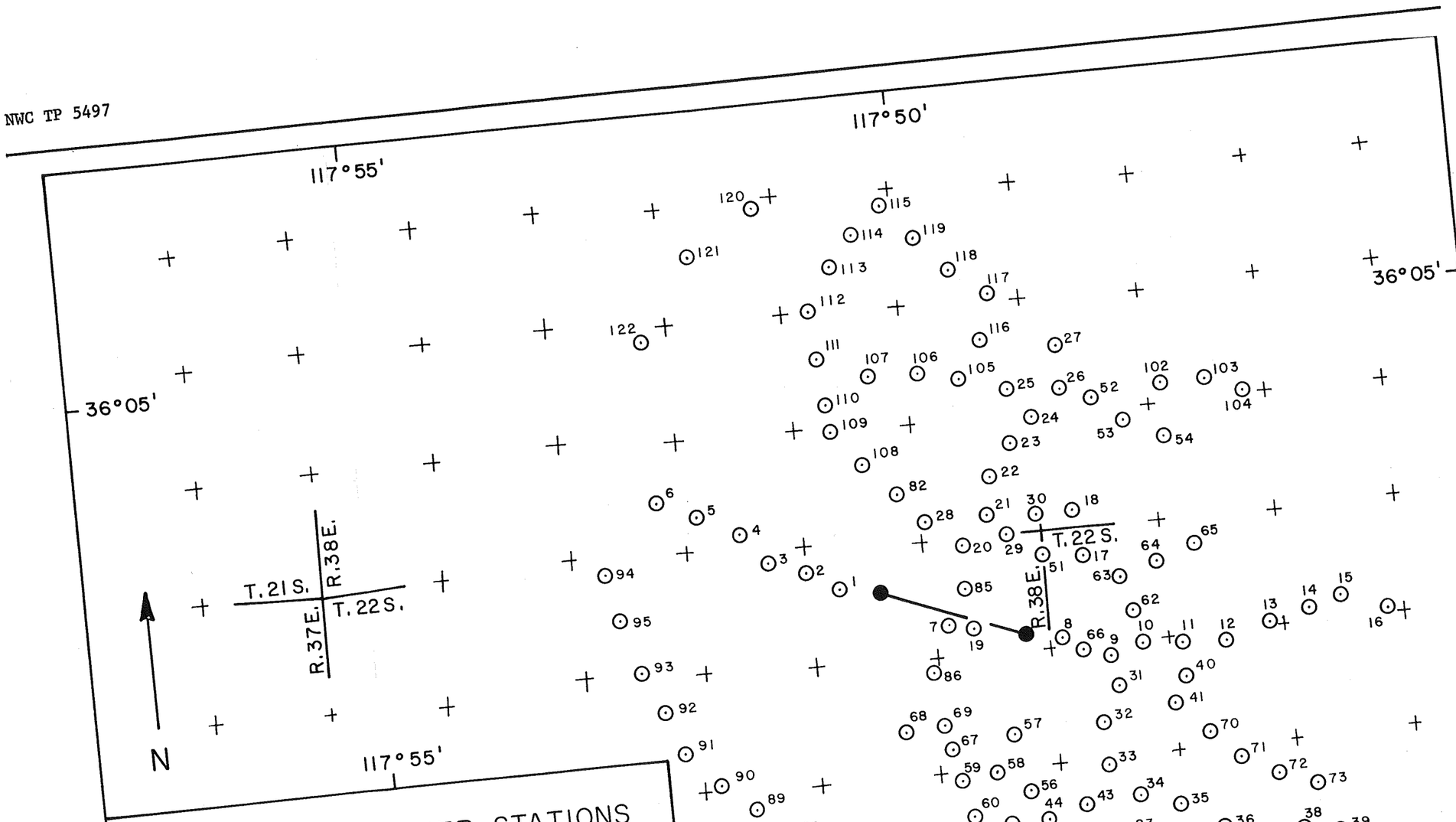

FIGURE 11: RECEIVER STATIONS MEASURED AROUND DIPOLE 1

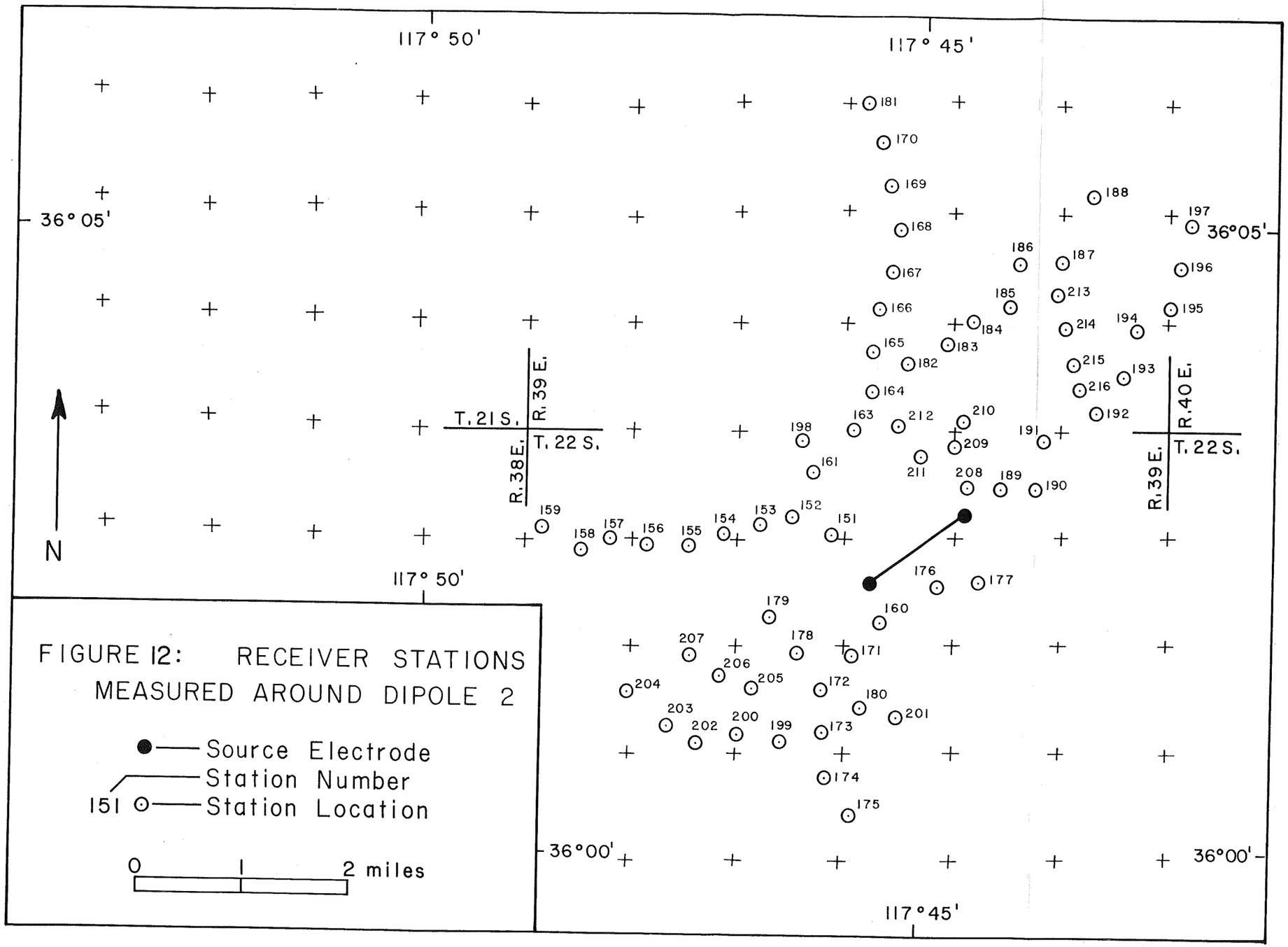

FIGURE 12: RECEIVER STATIONS MEASURED AROUND DIPOLE 2

● — Source Electrode

Station Number

151 ⊙ — Station Location

0 1 2 miles

with this formula are listed in Appendix B. These same data were used to compile the contour maps shown in Fig. 13 and 14.

A second common model is one where conductive rocks overlay a highly resistant substratum, such as crystalline basement rocks. For this layered model, the apparent resistivity increases linearly with distance from the source dipole for distances greater than the depth to the resistant rock. Since the current is constrained to flow almost entirely in the surface layer of conductive rock, the calculation of resistivity on the basis of an assumed spherical spreading of the current seems inappropriate. In this case, a more meaningful way to reduce the field data might be to use a formula based on the assumption of cylindrical spreading. For current spreading through a plate, the electric field depends on the ratio of plate thickness (h) to resistivity (ρ), h / ρ, a quantity which is also known as the conductance of the plate, S. The electric field at the surface of the plate for a current I to a single electrode is

$$E_1 = \frac{I}{2\pi S R_1}$$

where R_1 again is the distance from the first current electrode to the observation point. With the addition of a second electrode to complete the dipole current source, the contribution of a second electric field at the observation point must be considered

$$E_2 = \frac{-I}{2\pi S R_2}$$

The vector sum of these two electric fields is

$$E_T = \frac{I}{2\pi S R_1}\left[1 + \left(\frac{R_1}{R_2}\right)^2 - 2\left(\frac{R_1}{R_2}\right)\cos\delta\right]^{1/2}$$

Solving this expression for S provides the means for computing apparent conductance under the assumption of cylindrically symmetric spreading of current in a uniform conducting plate. Values for apparent conductance computed with this formula are also listed in Appendix B. These same data were used to compile the contour maps shown in Fig. 15 and 16.

EVALUATION OF THE SURVEY DATA

It must be stressed that the apparent values for resistivity or conductance calculated from dipole mapping data are the actual values

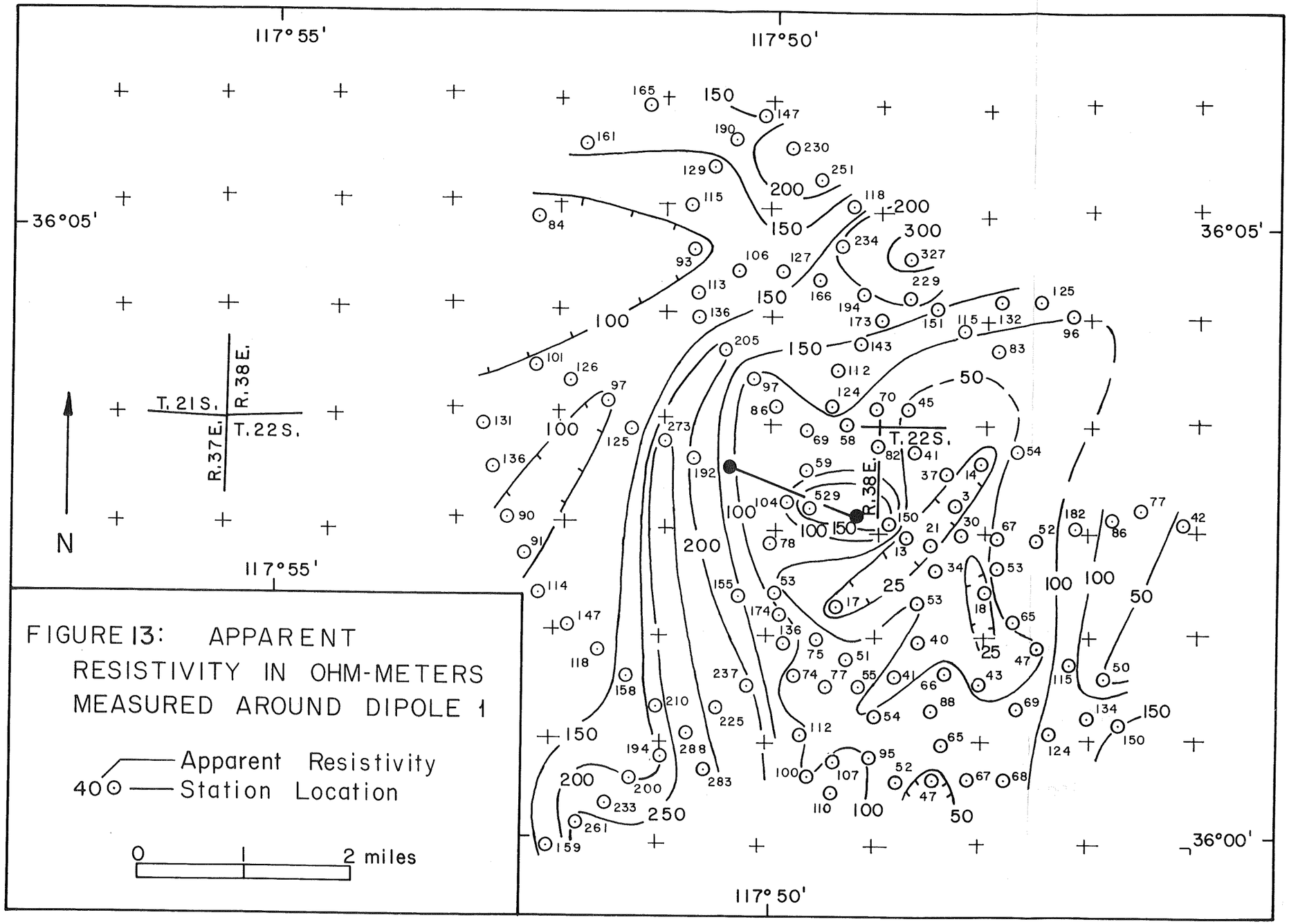
117°55'
117°50'
36°05'
36°00'
T. 21 S.
T. 22 S.
R. 37 E.
R. 38 E.
N
0
1
2 miles
Apparent Resistivity
Station Location
FIGURE 13: APPARENT RESISTIVITY IN OHM-METERS MEASURED AROUND DIPOLE 1

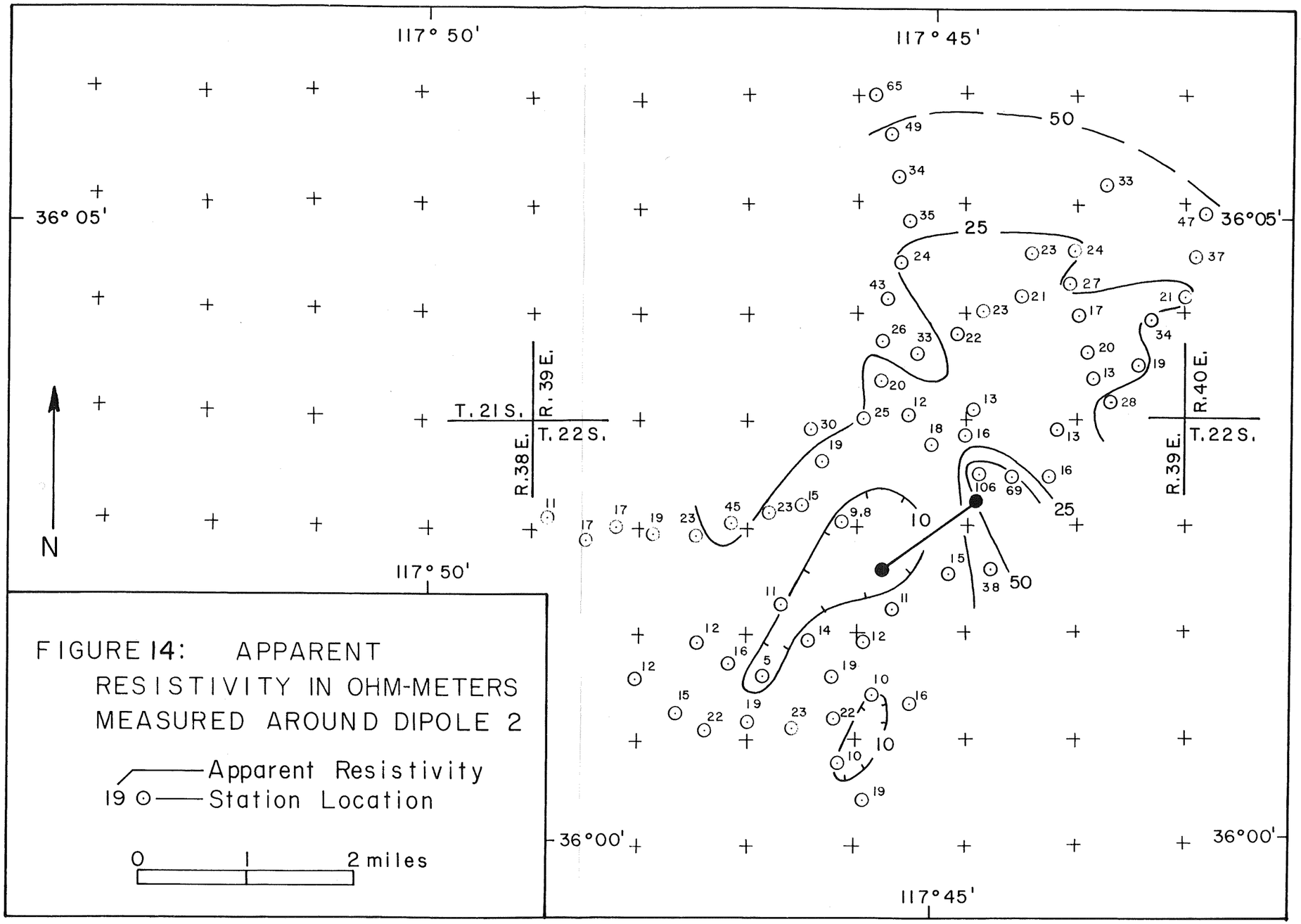

FIGURE 14: APPARENT RESISTIVITY IN OHM-METERS MEASURED AROUND DIPOLE 2

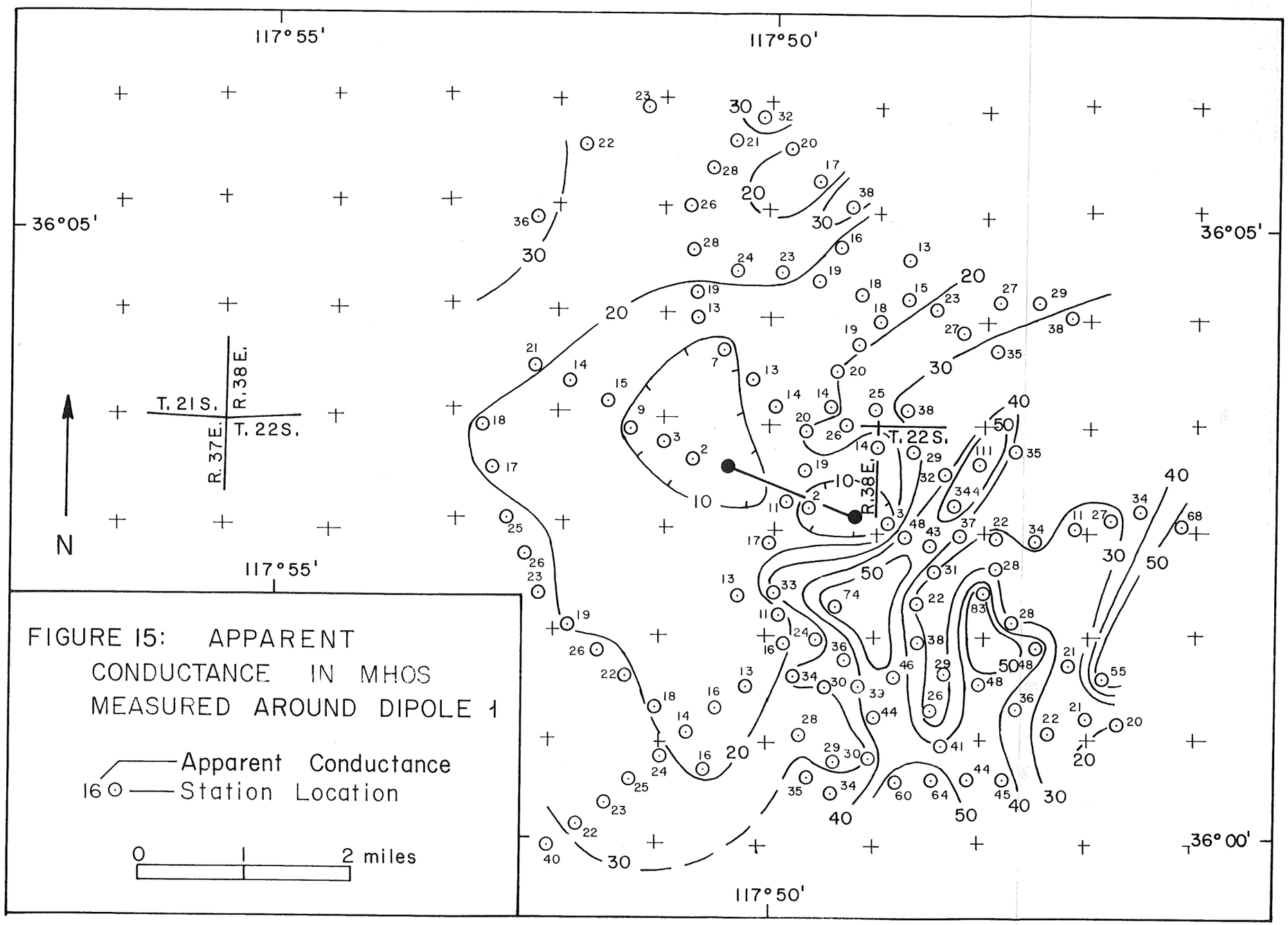
117°55'
117°50'
36°05'
36°00'
T. 21 S.
T. 22 S.
R. 37 E.
R. 38 E.
N
FIGURE 15: APPARENT CONDUCTANCE IN MHOS MEASURED AROUND DIPOLE 1
Apparent Conductance
Station Location
16
0
1
2 miles

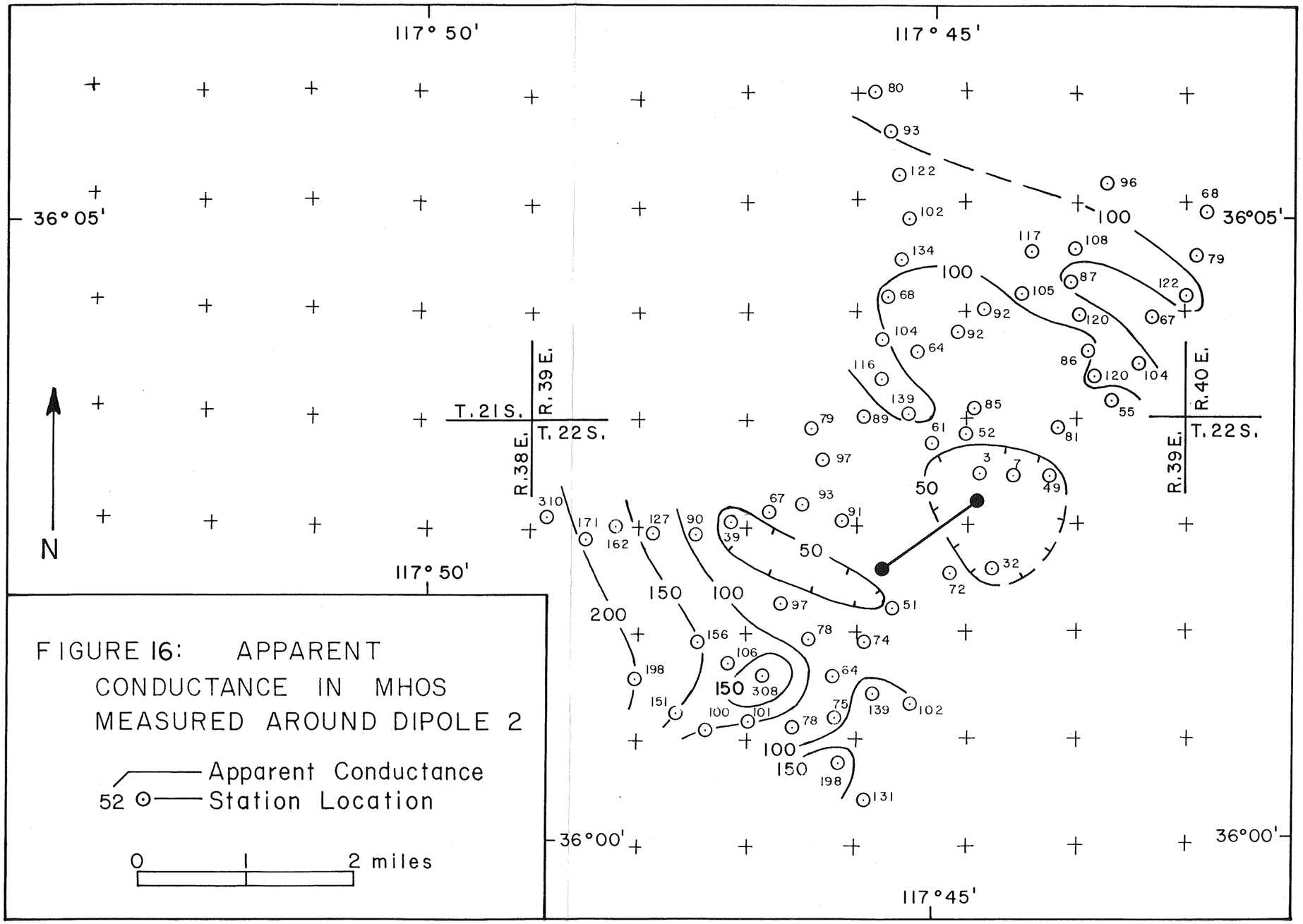

FIGURE 16: APPARENT CONDUCTANCE IN MHOS MEASURED AROUND DIPOLE 2

Apparent Conductance

52 Station Location

0 1 2 miles

only in the case in which the structure of the earth is as simple as that assumed in defining these quantities. That is, the earth must be completely uniform laterally. However, if a conductive geothermal reservoir is present in the survey area, we expect this condition to be violated. The computed values of apparent resistivity and apparent conductance will be functions of any lateral changes in resistivity which are present, but it is unlikely that the observed values will be close to the values actually existing in the ground. As a result, it is desirable to calculate how the apparent values are affected by simple models of laterally inhomogeneous earth structures.

The calculation of apparent resistivity is based on the model of a completely uniform earth. In many survey areas, in addition to the anomalous conductivity associated with a geothermal cell, there is a marked contrast in resistivity between the porous section in which the geothermal reservoir exists and the underlying basement. For measurements made at distances from the source greater than the depth to basement, the apparent resistivity value computed from the field measurements mainly reflects the higher basement resistivity. When this effect is present, apparent resistivity contours form an elliptical pattern about the source (see Fig. 17). The eccentricity of the ellipses reflects the well-known fact that measurements made along the polar axis of a dipole source do not detect the presence of a resistant basement until larger spacings are reached than are required when measurements are made along the equatorial axis (Keller, Ref. 16). It should also be noted that there are two small regions about the ends of the dipole where the apparent resistivity is lower than unity, the resistivity assigned to the surface layer. The elliptic behavior makes it more difficult to see the patterns in resistivity which may be associated with local anomalies such as are present in geothermal cells, and in addition, makes it difficult to superimpose measurements made from different dipole sources on a common map.

This problem for the layered model can be eliminated to a considerable degree by using the apparent conductance values, computed on the assumption that current spreads through a conducting plate. The thickness of the plate (that is, the thickness of the porous part of the section) need not be known, if the distance at which measurements are made is greater than the plate thickness. In contrast to the large variations in apparent resistivity as a function of distance from the source, the values of apparent conductance show very little change over most of the map (Fig. 18), after reaching some 98 percent of the correct value of S for the surface layer at a distance of about one unit from the dipole. The shape of the contours several source lengths away from the source are roughly hyperbolic.

On the maps for Source 1 (Fig. 13 and 14), there is an abrupt decrease in the apparent resistivity (hereafter designated RA) and an abrupt increase in apparent conductance (hereafter designated SA) to the

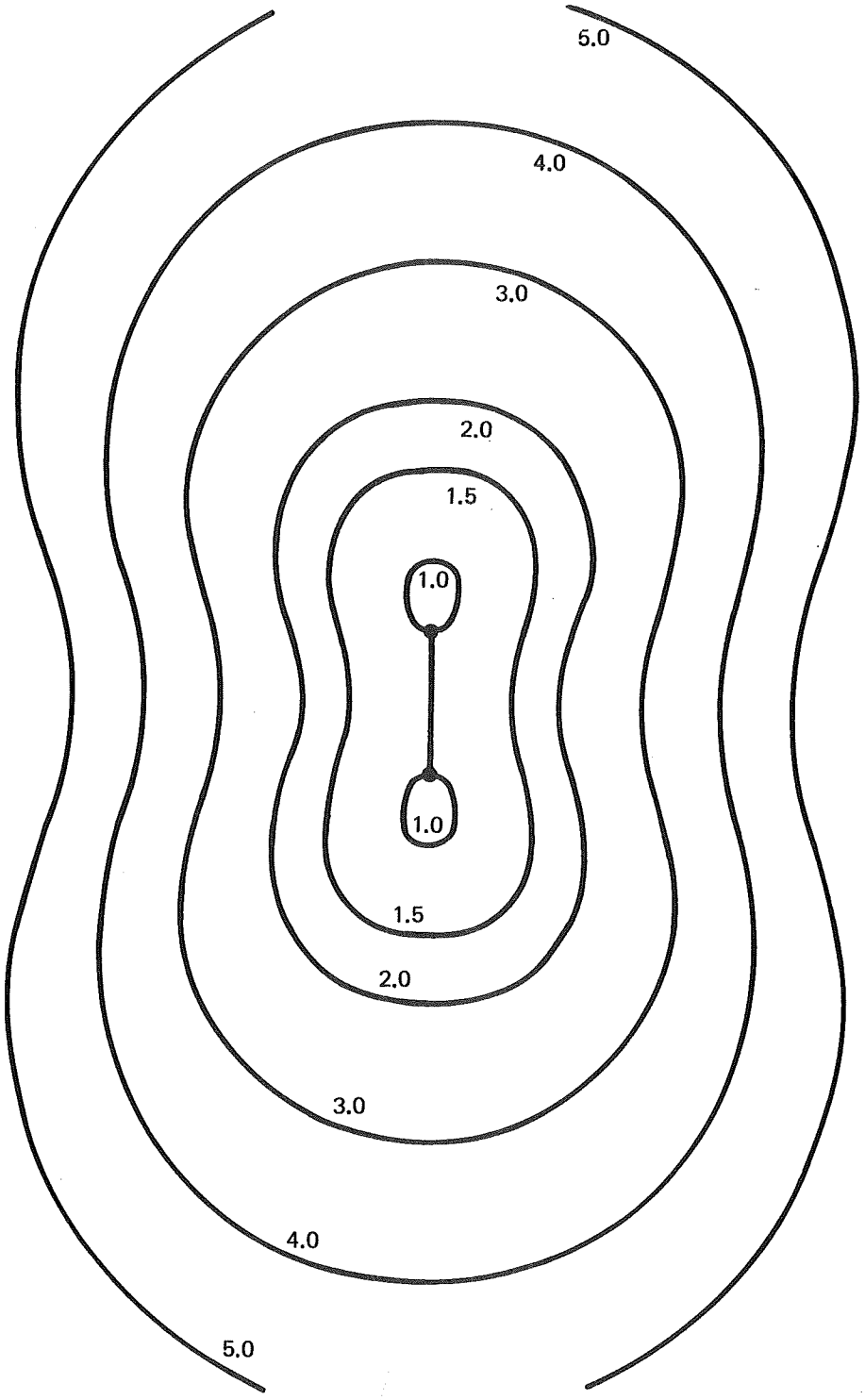

FIG. 17. Apparent Resistivity Dipole Map for the Case of a Two Layer Sequence in Which the Surface Layer has Unit Resistivity, the Second Layer Resistivity is 1000 times that of the First Layer, and the Thickness of the First Layer is Half of the Source Dipole Length. (From Furgerson and Keller, Ref. 25.)

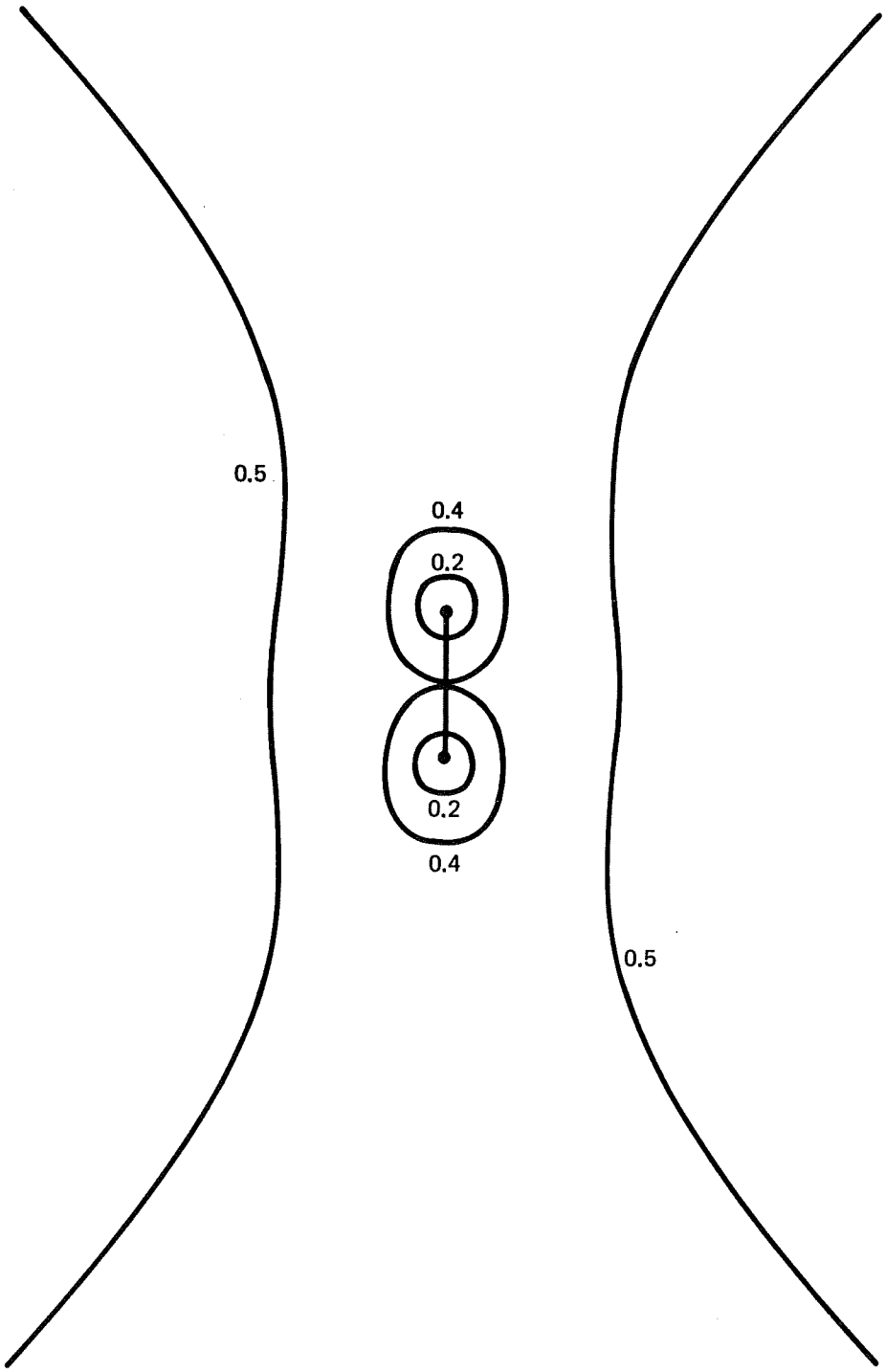

FIG. 18. Apparent Conductance Dipole Map for the Case of a Two Layer Sequence in Which the Surface Layer has Unit Resistivity, the Second Layer resistivity is 1000 Times That of the First Layer, and the Thickness of the First Layer is Half of the Source Dipole Length.
(From Furgerson and Keller, Ref. 25.)

southeast of a northeast-southwest line passing through the southeastern electrode of Source 1. For Source 2 (Fig. 15 and 16), there is a roughly elliptical character to the RA contours and a roughly hyperbolic character to the SA contours, behavior which suggests the presence of a reasonably thick conductive section with a resistive basement covering much of the area southeast of the line mentioned above. The major exception is a somewhat resistive ridge separating the Devil's Kitchen-Nicol area and the Coso Hot Springs-Wheeler area.

Perhaps a better model for this case would be one which combines both the lateral change and the layered sequence described above. Such models are being prepared by Furgerson and Keller (Ref. 25). The selection of finished maps is not large, but enough are available to make interesting comparisons with field data. Figures 19 and 20 show the SA maps for a vertical contact between two media of different conductances lying on a resistive basement. Figure 19 shows the source dipole in the more conductive medium, and Fig. 20 shows it in the less conductive medium. The source dipole is oriented normal to the vertical contact with its center located 3 dipole lengths from the contact; the contrast in conductance across the contact is ten. Only the SA maps are shown because SA usually gives less complex maps than RA when a layered sequence is present. The source's distance from the contact and its angle with the contact are ill-matched in these examples compared to the field maps, but the important characteristics are still present. They show that a sharp lateral change in conductance is more easily seen when the source electrodes are on the less conductive side of the contact; i.e., for this example, the average contrast across the contact is 5 when the source is in the less conductive medium (Fig. 20) and 2 when it is in the more conductive medium (Fig. 19). Another feature is that the apparent conductance on the far side of the contact, S_F, is given by

$$S_F = \frac{S_2}{1-K_s}$$

where S_1, S_2 = true conductance on the near side and the far side of the contact, respectively,

and

$$K_s = \frac{S_1 - S_2}{S_1 + S_2}$$

Thus the apparent conductance on the far side of the contact is larger than the true value when the source electrodes are on the more conductive side of the contact and less than the true value when the source electrodes are on the less conductive side of the contact. By using the above formula and applying it to field maps, it should be possible to calculate true regional conductances on both sides of the contact. Such calculations will be made when sufficient areas have been covered with both

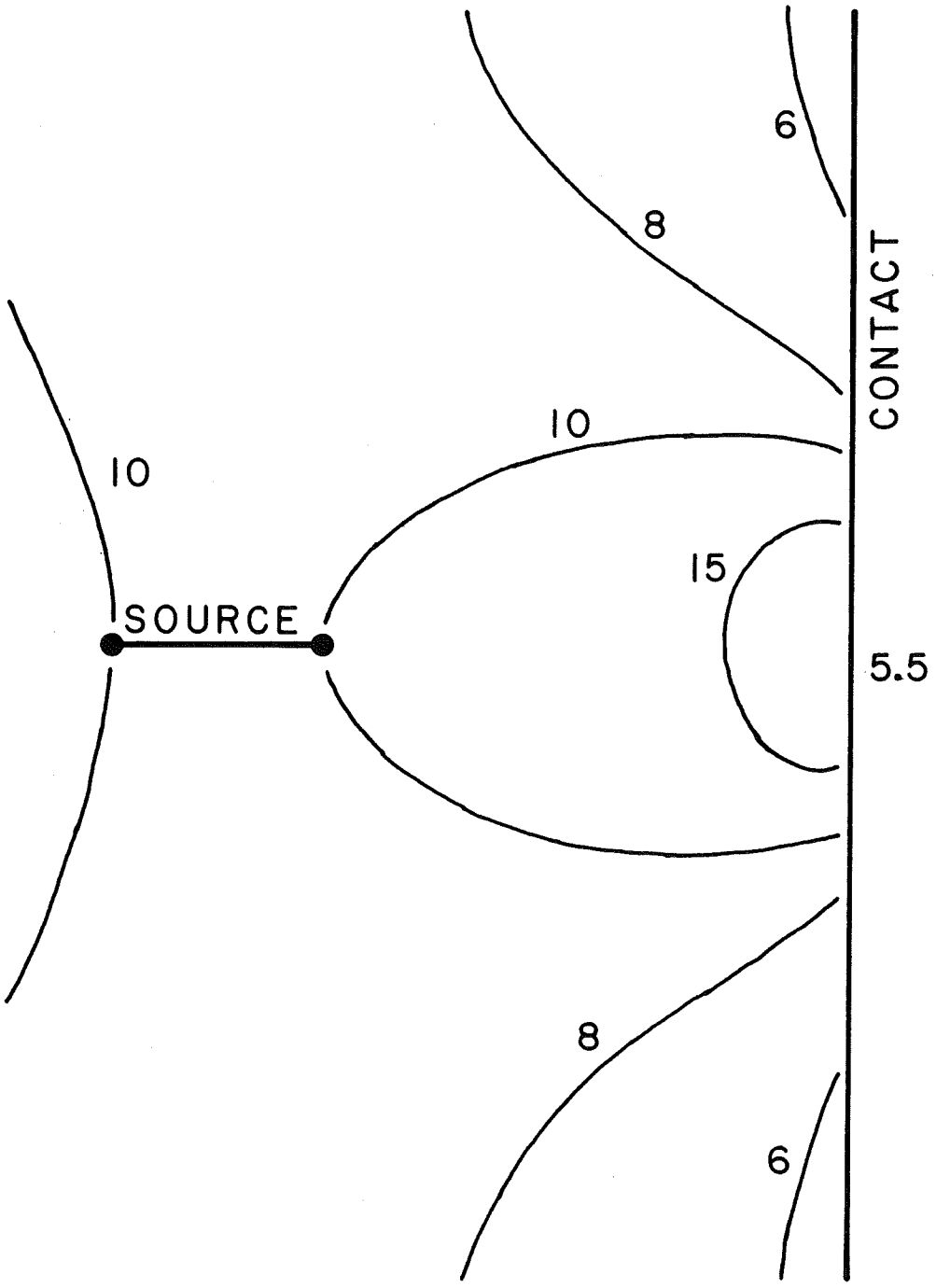

FIG. 19. Apparent Conductance Dipole Map for the Case of a Vertical Contact Between Two Media Which have a Conductance Contrast of 10 and Lie on a Resistive Basement. The source dipole has unit length and is in the more conductive medium. (From Furgerson and Keller, Ref. 25.)

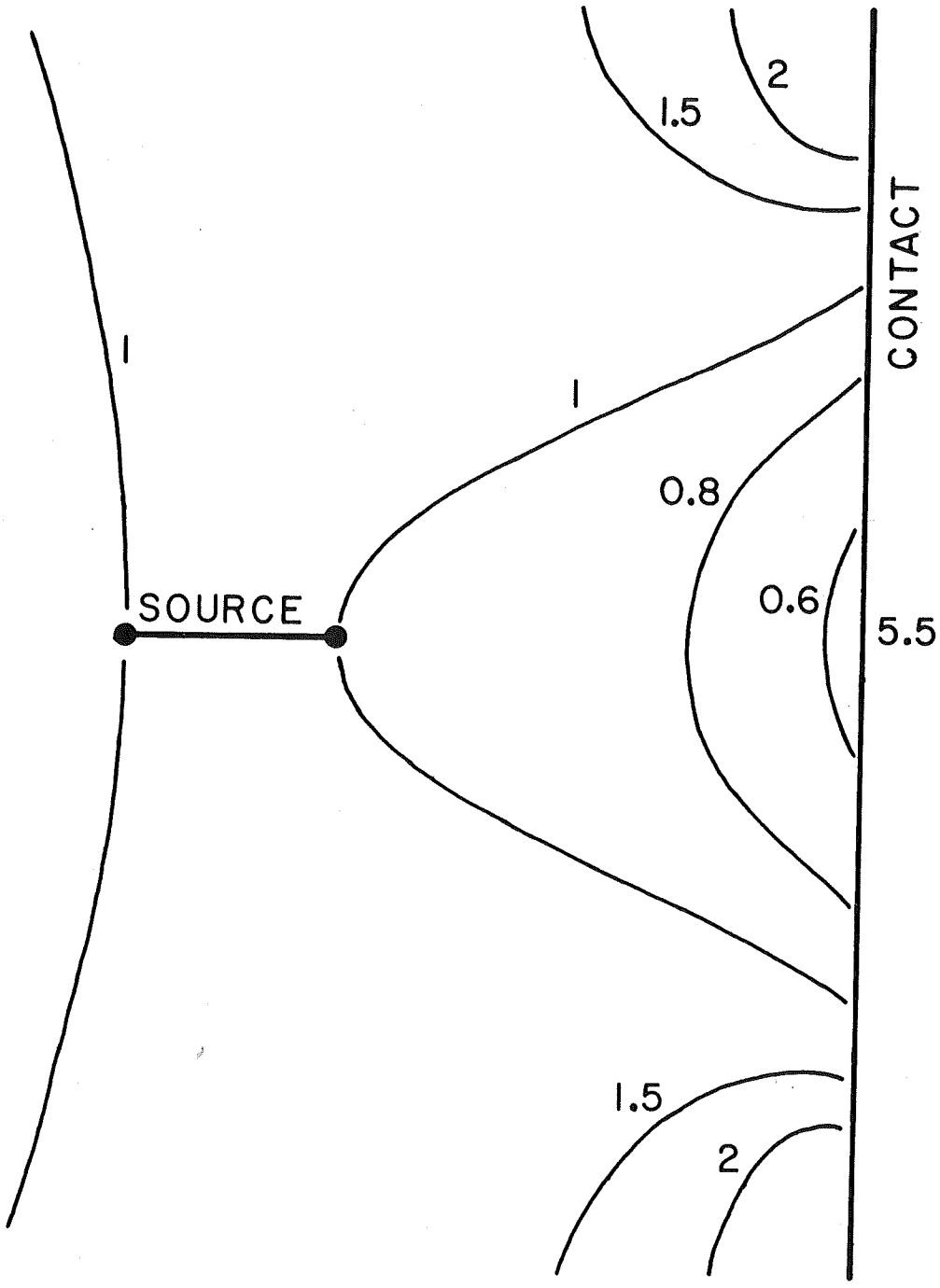

FIG. 20. Apparent Conductance Dipole Map for the Case of a Vertical Contact Between Two Media Which have a Conductance Contrast of 10 and Lie on a Resistive Basement. The Source dipole has unit length and is in the less conductive medium.
(From Furgerson and Keller, Ref. 25.)

Electric fields were measured at distances from a source dipole ranging up to 4 miles. Measurements were usually not made closer than about one-half mile from the end of a source dipole, because an advantage in using the dipole mapping technique lies in the capacity to make measurements at sufficient distance to assure penetration to depths of many thousands of feet. Measurements made close to one end of a dipole source will reflect the resistivity only to a shallow depth, comparable to the distance from the end of the line. Several dipole sources are being used to provide adequate coverage and to insure a reasonable amount of overlap so that areas which appear to be promising will be covered with measurements made from more than one source. So far about 200 measurements have been made around two sources (see Fig. 11 and 12 for location maps), and the primary data obtained are listed in Appendix B. These data may be converted to apparent resistivity values using several different formulas.

The conventional manner of defining apparent resistivity is to consider what resistivity a uniform earth would require to provide the voltages actually measured. In a uniform earth, current spreads out from a single electrode with spherical symmetry. The electric field strength on the surface of the earth at a distance R_1 from a single electrode through which a current I is passing is then

$$E_1 = \frac{\rho I}{2\pi R_1^2}$$

where ρ is the resistivity of the assumed uniform earth. When a dipole pair of electrodes is used for a current source, there is a second contribution to the electric field from the current flowing through the second electrode:

$$E_2 = \frac{\rho I}{2\pi R_2^2}$$

where R_2 is the distance from the observation point to the second current electrode. The electric fields E_1 and E_2 are vector quantities, and must be added vectorially. The vector sum is

$$E_T = \frac{\rho I}{2\pi R_1^2}\left[1 + \left(\frac{R_1}{R_2}\right)^4 - 2\left(\frac{R_1}{R_2}\right)^2 \cos\delta\right]^{1/2}$$

Solving this expression for ρ provides the means for computing apparent resistivity under the assumption of spherically-symmetric spreading of current in a uniform earth. Values for apparent resistivity computed

Electric fields were measured at distances from a source dipole ranging up to 4 miles. Measurements were usually not made closer than about one-half mile from the end of a source dipole, because an advantage in using the dipole mapping technique lies in the capacity to make measurements at sufficient distance to assure penetration to depths of many thousands of feet. Measurements made close to one end of a dipole source will reflect the resistivity only to a shallow depth, comparable to the distance from the end of the line. Several dipole sources are being used to provide adequate coverage and to insure a reasonable amount of overlap so that areas which appear to be promising will be covered with measurements made from more than one source. So far about 200 measurements have been made around two sources (see Fig. 11 and 12 for location maps), and the primary data obtained are listed in Appendix B. These data may be converted to apparent resistivity values using several different formulas.

The conventional manner of defining apparent resistivity is to consider what resistivity a uniform earth would require to provide the voltages actually measured. In a uniform earth, current spreads out from a single electrode with spherical symmetry. The electric field strength on the surface of the earth at a distance R_1 from a single electrode through which a current I is passing is then

$$E_1 = \frac{\rho I}{2\pi R_1^2}$$

where ρ is the resistivity of the assumed uniform earth. When a dipole pair of electrodes is used for a current source, there is a second contribution to the electric field from the current flowing through the second electrode:

$$E_2 = \frac{\rho I}{2\pi R_2^2}$$

where R_2 is the distance from the observation point to the second current electrode. The electric fields E_1 and E_2 are vector quantities, and must be added vectorially. The vector sum is

$$E_T = \frac{\rho I}{2\pi R_1^2}\left[1 + \left(\frac{R_1}{R_2}\right)^4 - 2\left(\frac{R_1}{R_2}\right)^2 \cos\delta\right]^{1/2}$$

Solving this expression for ρ provides the means for computing apparent resistivity under the assumption of spherically-symmetric spreading of current in a uniform earth. Values for apparent resistivity computed

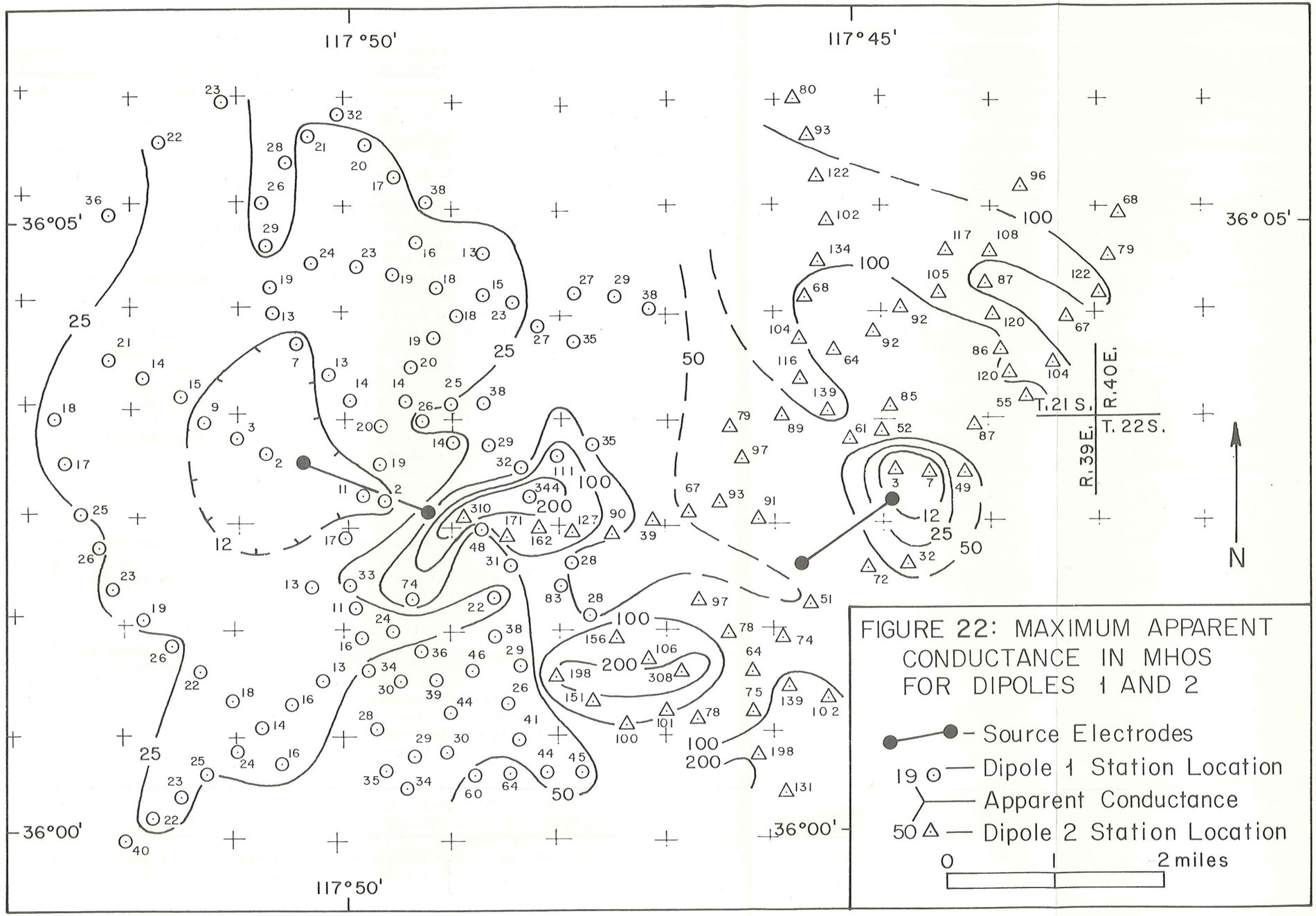

FIGURE 22: MAXIMUM APPARENT CONDUCTANCE IN MHOS FOR DIPOLES 1 AND 2

- Source Electrodes
- 19 ⊙ — Dipole 1 Station Location
- Apparent Conductance
- 50 △ — Dipole 2 Station Location

Sounding HR-8 was set up in the center of, and expanded parallel to, Source 1. The Schlumberger sounding can be "expanded" to larger separations by calculating bipole-dipole equatorial resistivities from dipole mapping measurements made reasonably close to the perpendicular bisector of Source 1. According to Zohdy and Jackson (Ref. 27), Berkichevskii and Petrovskii (Ref. 28) have shown that a bipole-dipole equatorial sounding curve is identical to a Schlumberger sounding curve for a horizontally stratified, laterally-homogeneous medium. The interpretation given in Appendix A shows that the conductive section is at least 1400 ft thick under a thin surface layer of unconsolidated alluvium (60 ft thick) and high resistivity (8400 ohm-m) volcanic pyroclastics. This sounding dramatically points up the limited penetration of a dipole mapping survey very near the source dipole. Therefore, the region of conductive ground noted at the beginning of this section probably extends some distance to the northwest under Source 1. The location of the western boundary of this conductive zone should be easily located when more stations are made from Source 2 with the larger current steps to be used. It should be stressed that the thickness estimate given above is a minimum value; as the electrode separation is increased there is a greater chance of the curve being affected by lateral inhomogeneities, in this case the high resistivity granitic bedrock exposed along the northeast and southwest lines of extension. Sounding HR-11 is very similar to HR-8; although the conductive zone appears to have a somewhat higher resistivity, it should be noted that the resistivity of 55 ohm-m for this section given in Appendix A is a maximum value. Also, there is no sign of a resistive basement on the sounding curve, which indicates that the conductive section is at least 3000 ft thick and possibly 12,000 ft or more thick.

Soundings C-3 and HR-2 indicate a conductive section with the same resistivity and general thickness as HR-8, but with the top at a greater depth (1600 to 2300 ft). The most logical explanation for the thick interval of high resistivity (250 to 500 ohm-m) above the conductive section in each sounding is that it represents cool, dry granitic host rock above a deep low-salinity geothermal reservoir. The first two layers indicate that the basalt flows beneath C-3 are approximately 160 ft thick with the upper 20 ft highly weathered. Sounding HR-7 appears to be similar to C-3 and HR-2, but the higher resistivity of 140 ohm-m for the deep interval indicates the sounding is probably off the edge of the heat source and that only moderate temperatures are present. The first two layers represent the partially eroded perlite dome on which the sounding was made.

Sounding HR-9 was made to investigate the sediments in the Rose Valley basin. The seismic and gravity interpretations by Healy and Press (Ref. 19) have already been discussed, and HR-9 supports the interpretation that the 2100 ft deep, high velocity arrival is not a basement arrival. The 5600 ft depth obtained from the gravity interpretation fits HR-9 very well. Not enough information is presently

available to determine whether the thick conductive section is indicative of high salinity groundwater flow from Owen's Valley or a geothermal reservoir. The first possibility is more likely but more work is needed to verify it.

The dipole maps (Fig. 13-6, 21, 22) and the Schlumberger sounding interpretations can be used quite effectively in locating or extending some of the faults and/or fractures which appear to control at least the surface geothermal emissions and probably the deeper portions of the reservoir as well. Figure 2 shows the faults and/or fractures interpreted from the electrical survey along with some taken from the literature (Moyle, Ref. 7, and Stenson, unpublished) and one interpreted by the author from air photos. Many of the volcanic cones lie along the faults and their junctions, and several through-going faults are visible. One starts in Sec. 2, T.23S., R.38E. and winds north and northeast through Devil's Kitchen and the Nicol prospect to Sec. 33, T.21S., R.39E. Another starts in Sec. 29, T.22S., R.39E. and trends north-northwest into the middle of the perlite dome complex of Sugarloaf and probably extends through the north-south group of perlite domes into Sec. 24, T.21S., R.38E. where Stenson (unpublished mapping) has mapped a north-south fault.

CONCLUSIONS AND RECOMMENDATIONS

Recalling that a GRI of 5 or more is needed under normal circumstances for a promising geothermal system and that, according to interpretations of the Schlumberger soundings, the cold granitic host rock has a resistivity of 250 ohm-m or more, it appears that areas with sections having resistivities below 50 ohm-m should be examined in detail. This includes most of the surveyed area southeast of a line connecting dipole mapping stations 170, 65, 18, 29, 69 and 48 (Fig. 11 and 12). The conductive section appears to vary considerably in thickness from about 700 ft thick to possibly 12,000 ft or more thick. The dipole maps are extremely effective in mapping faults and fractures which should be very useful in selecting porous and permeable drilling targets.

After measurements have been completed around Sources 1 and 2, two more source locations are recommended. The most important would be one located to the south of Sources 1 and 2 to find the boundaries of the conductive section in that direction. One possible location is Sections 28 and 34 at the north end of Airport Lake. The second new source location would be to the north of Sources 1 and 2 to find the boundaries of the conductive section to the northeast of Source 2. One possible location is Sec. 15, T.21S., R.39E.

To better determine the vertical extent of the conductive section, more Schlumberger soundings and some electromagnetic soundings should be made. The electromagnetic soundings can use the dipole mapping source dipoles as sources to achieve penetration depths of 2 miles or more and are less affected by lateral changes in resistivity than are Schlumberger soundings. Another advantage of electromagnetic sounding is that the receiver can be a short (1500 ft) multi-turn loop instead of long potential measuring wires used in the Schlumberger sounding technique.

Another recommendation is to try to determine whether the thick, low resistivity section found in Rose Valley is a potential geothermal reservoir or merely cold, high-salinity groundwater flow out of Owen's Valley. One possible method is to make temperature gradient measurements in the Coso Junction water well.

The great potential value of high altitude aerial photography in mapping structural features associated with geothermal systems has been stressed by Austin and others (Ref. 9). Such photos should become available soon after the launch of the next Earth Resources Technology Satellite (ERTS) which is tentatively scheduled for late 1973, and it is recommended that access to them be obtained and a detailed interpretation be made.

APPENDIX A

This appendix contains the Schlumberger electrical resistivity soundings made in the Coso Geothermal Area. The field data are represented by points enclosed in open circles. The theoretical curve deemed the best interpretation is represented by a solid line. Resistivity-depth information obtained from the dipole mapping surveys are indicated by dashed lines. A 45-degree line is drawn on the sounding curve corresponding to the apparent conductance (SA) value in mhos, a horizontal line is drawn corresponding to the apparent resistivity (RA) value in ohm-meters, and a vertical line is drawn corresponding to the distance from the end of the dipole source in feet. A tabulation of interpretations corresponding to the theoretical curves follows.

Station Number	Resistivity in ohm-meters	Depth to Bottom of Layer in Feet
C-3	115	20
	4500	160
	500	1600
	50	
HR-1	23	5.6
	120	34
	23	150
	4.2	600
	12	2300
	95	
HR-2	200	150
	40	650
	250	2600
	65	

Station Number	Resistivity in ohm-meters	Depth to Bottom of Layer in Feet
HR-4	107	70
	2230	110
	212	
HR-5	215	300
	1100	450
	250	
HR-6	145	340
	1500	475
	230	
HR-7	825	20
	3000	125
	400	1800
	140	
HR-8	210	60
	8400	180
	20	1400
	2000	
HR-9	630	70
	125	350
	15	1680
	7	

Station Number	Resistivity in ohm-meters	Depth to Bottom of Layer in Feet
HR-10	20	2
	1000	24
	41	166
	4.6	700
	250	
HR-11	770	13
	2000	210
	55	

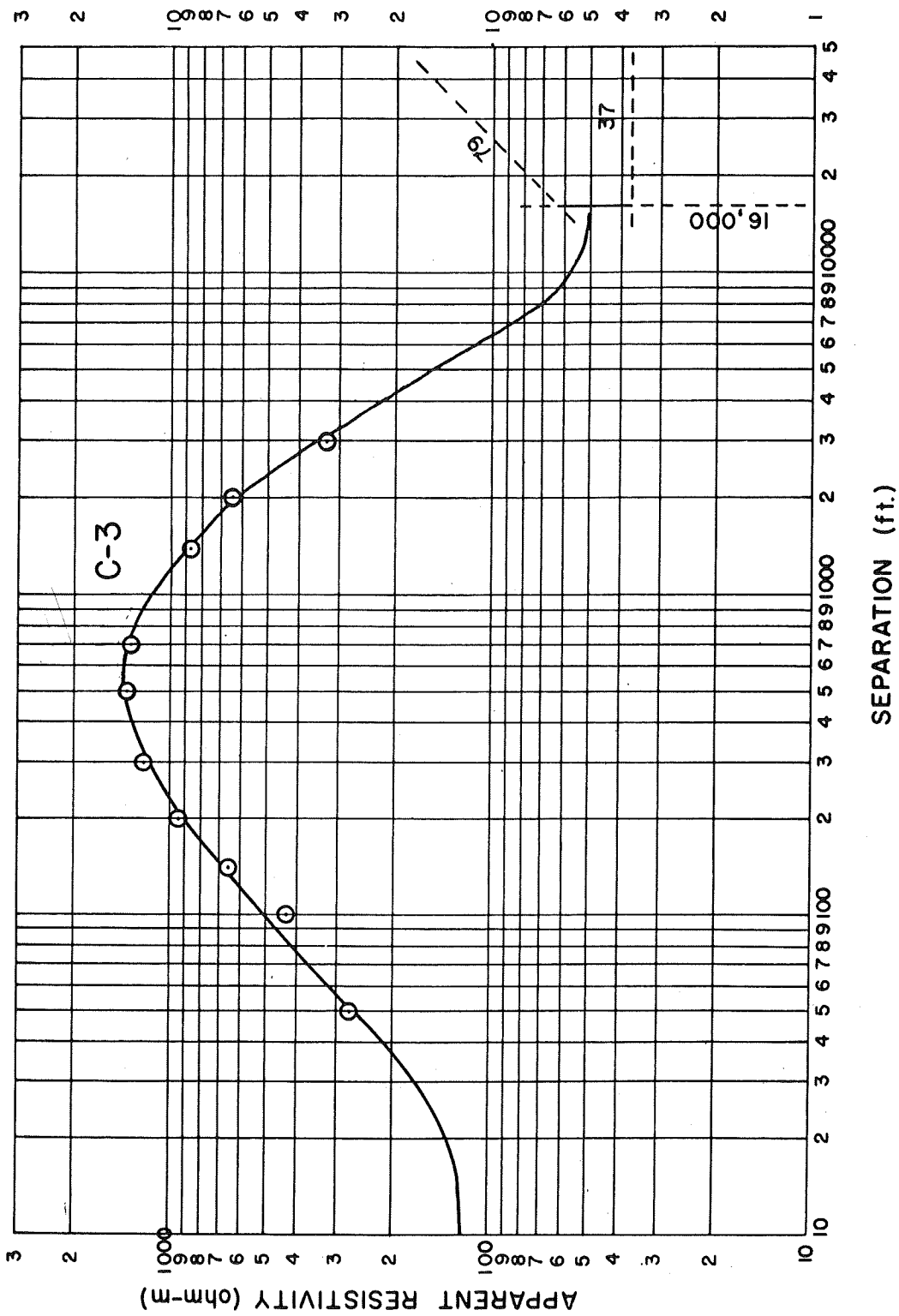
C-3
37
16,000
APPARENT RESISTIVITY (ohm-m)
SEPARATION (ft.)

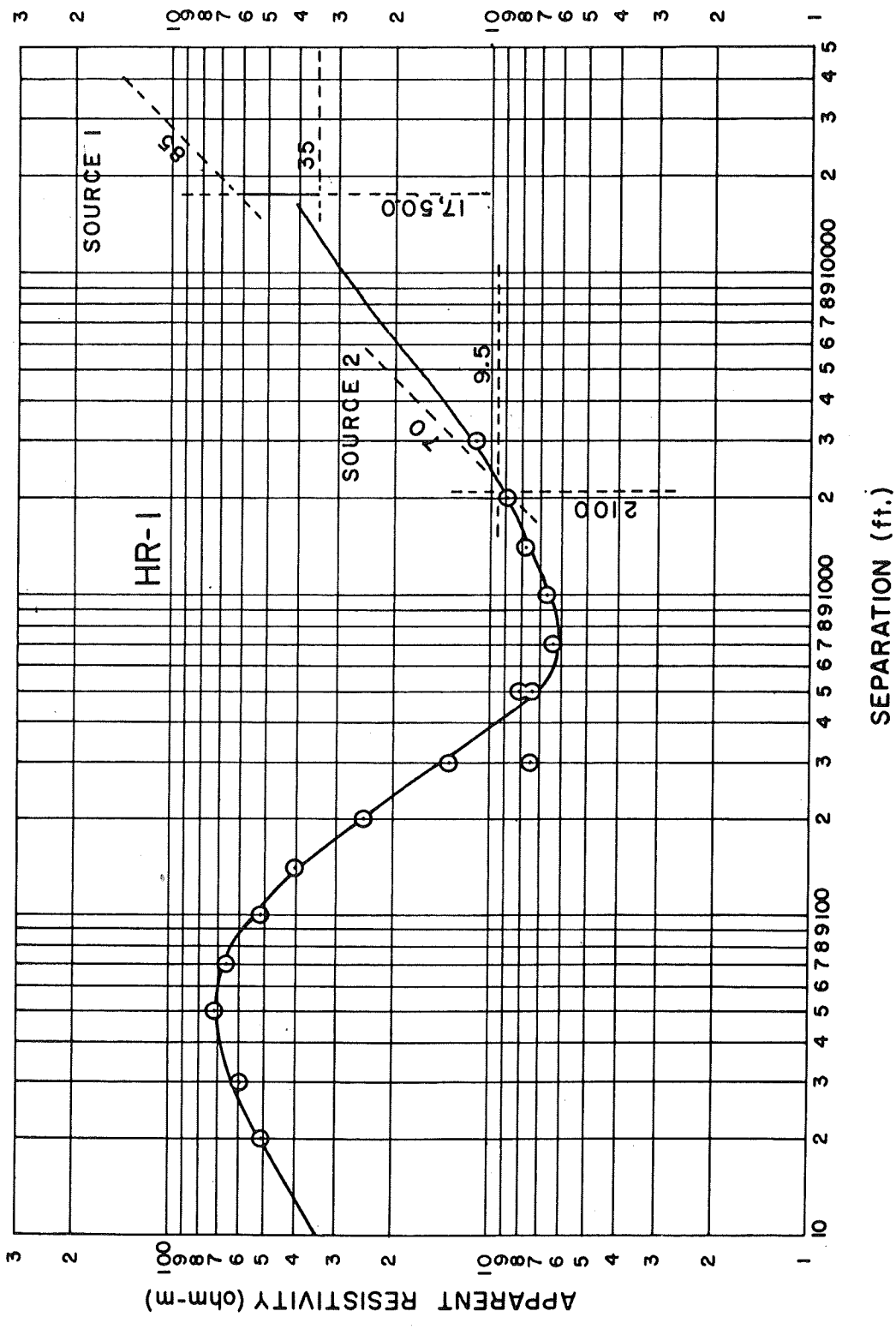
HR-1
SOURCE 1
SOURCE 2
5
8
35
17,500
1
0
9.5
2100
APPARENT RESISTIVITY (ohm-m)
SEPARATION (ft.)

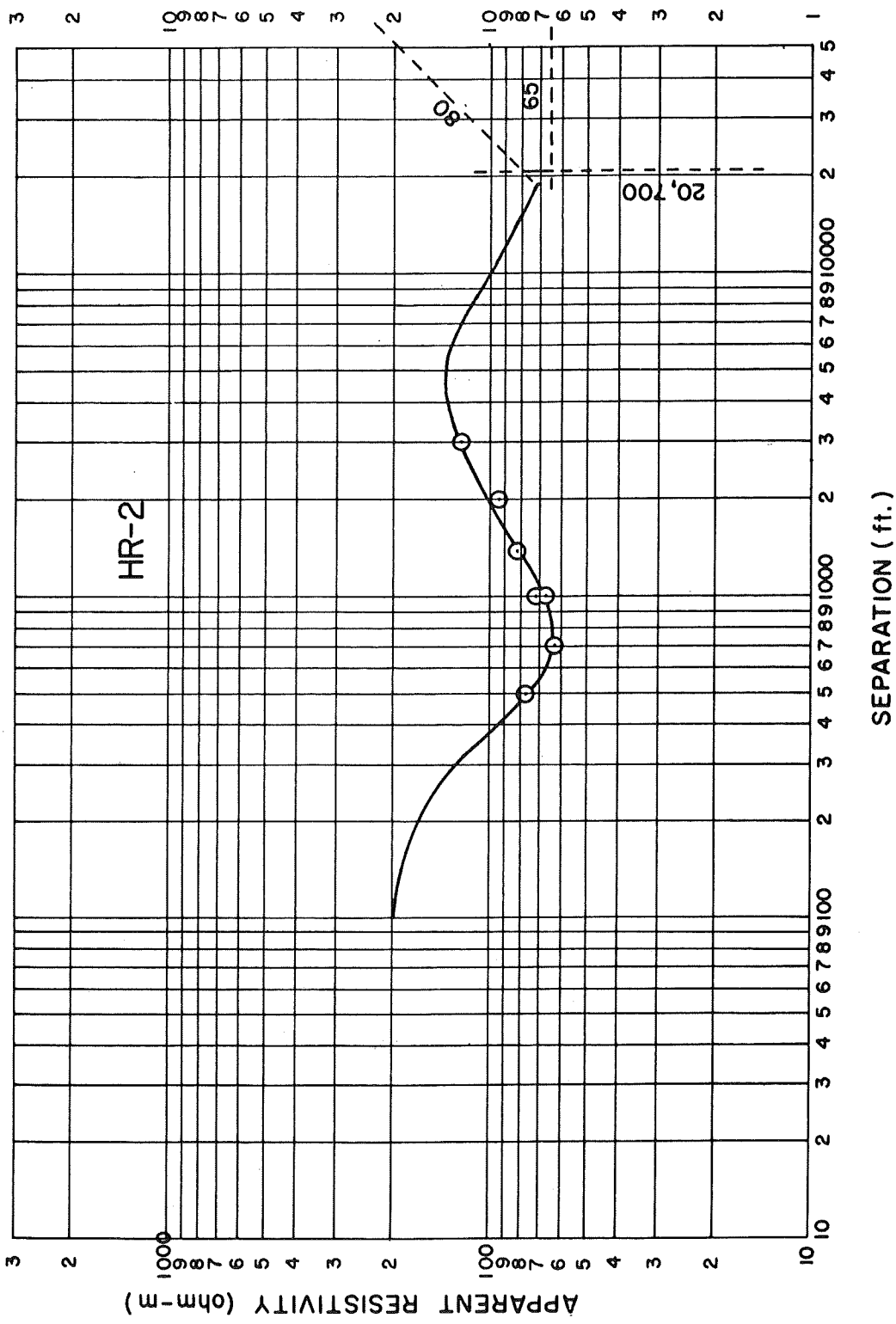
HR-2
90
65
20,700
APPARENT RESISTIVITY (ohm-m)
SEPARATION (ft.)

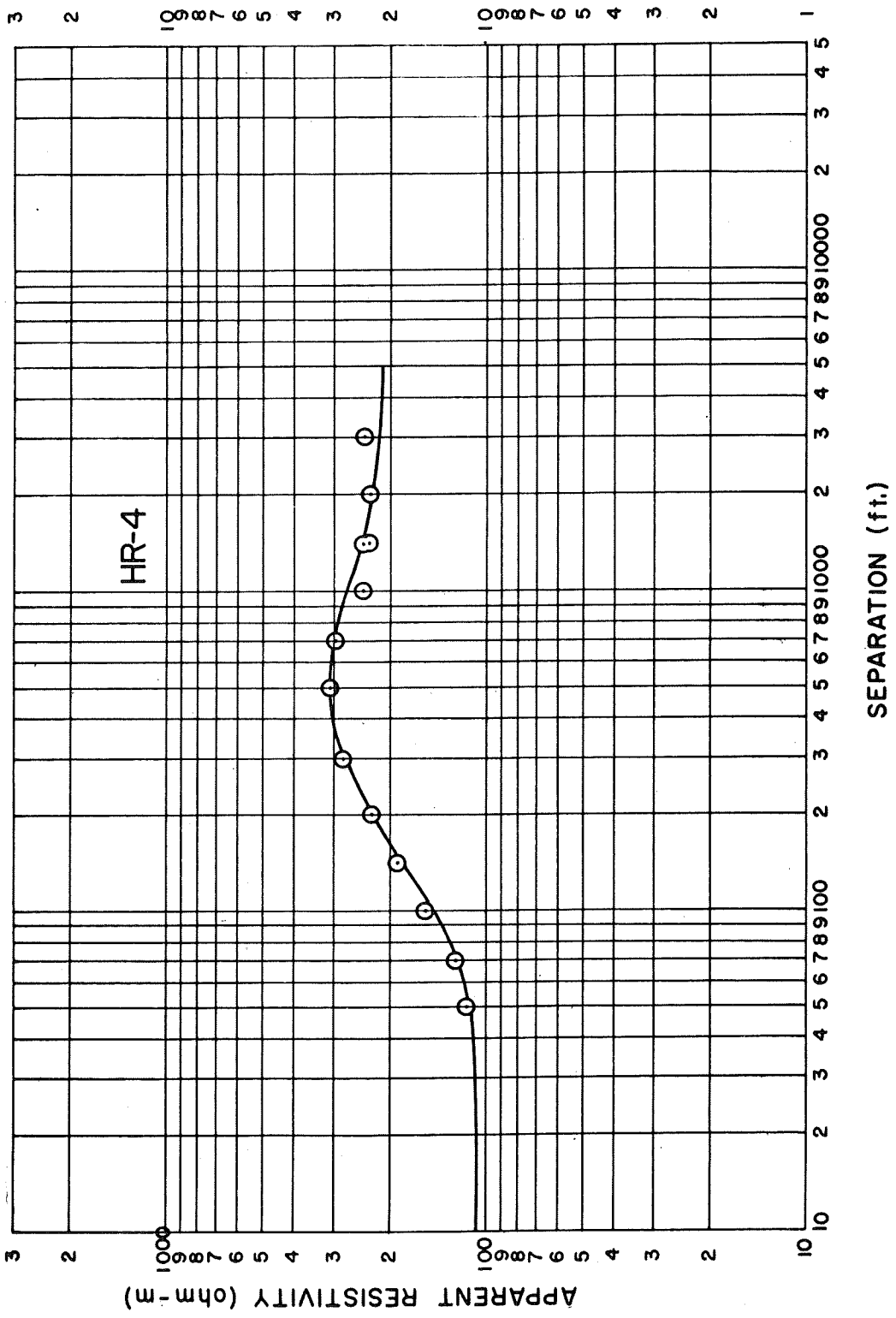
HR-4
APPARENT RESISTIVITY (ohm-m)
SEPARATION (ft.)

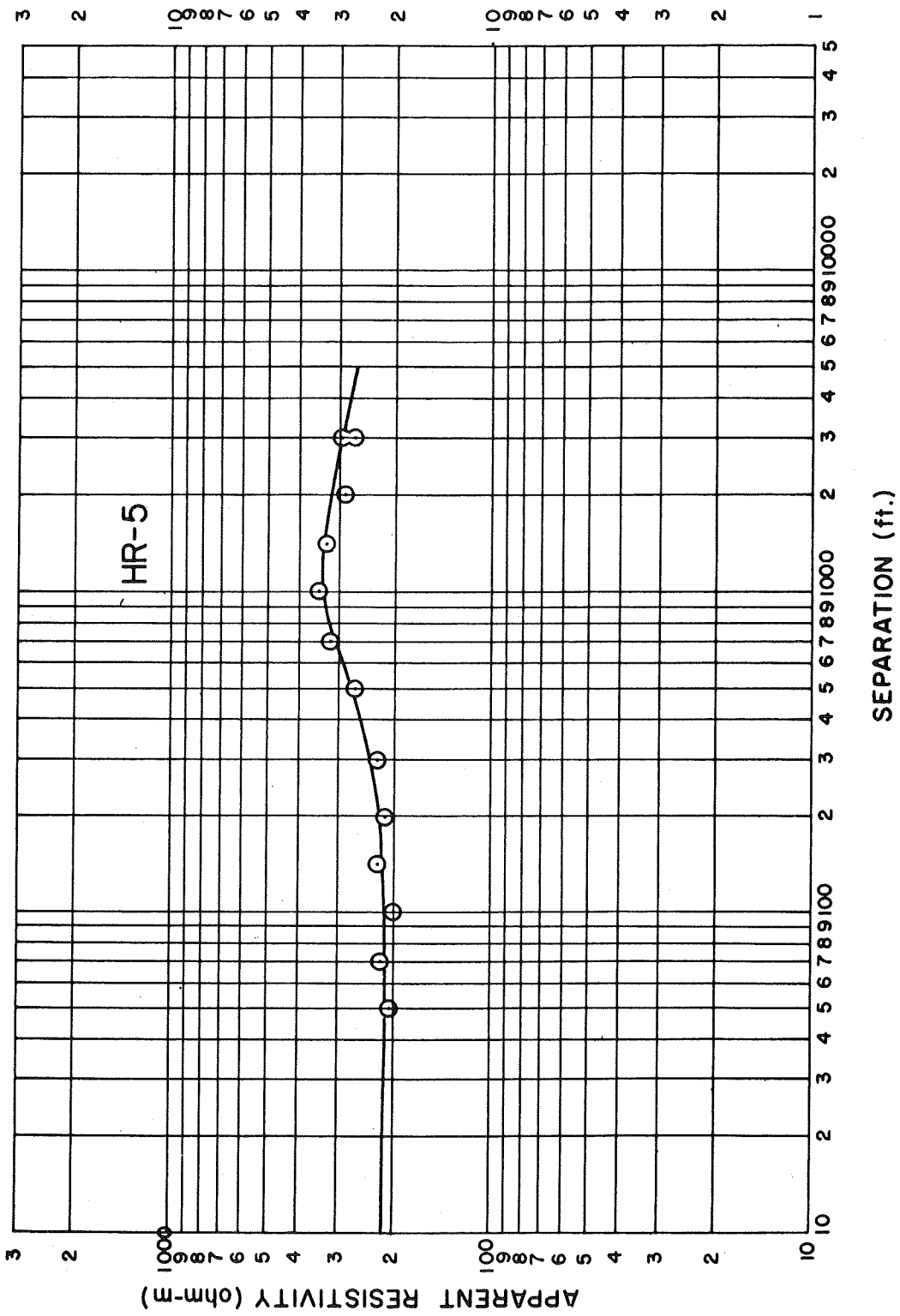
HR-5
APPARENT RESISTIVITY (ohm-m)
SEPARATION (ft.)

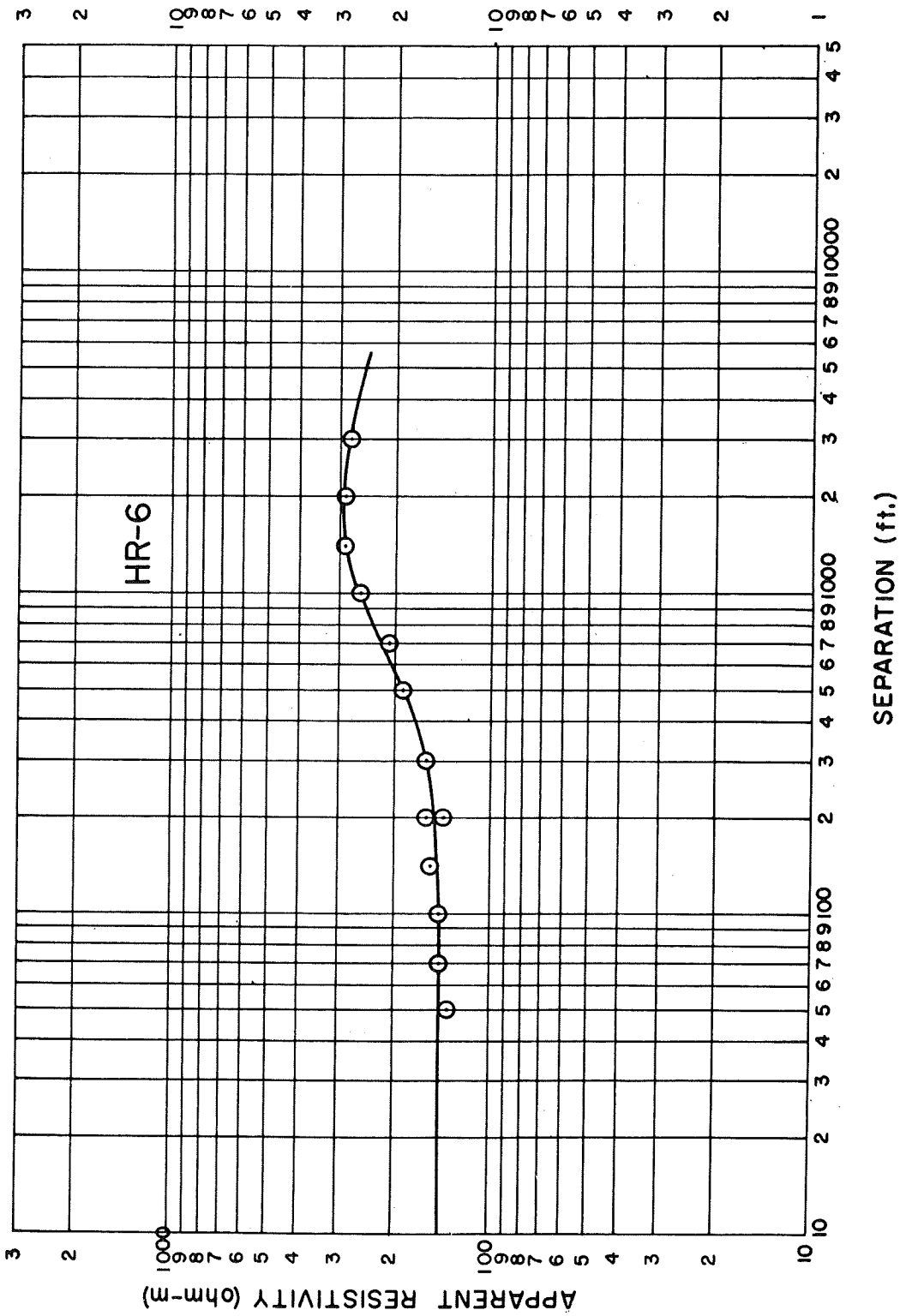
HR-6
APPARENT RESISTIVITY (ohm-m)
SEPARATION (ft.)

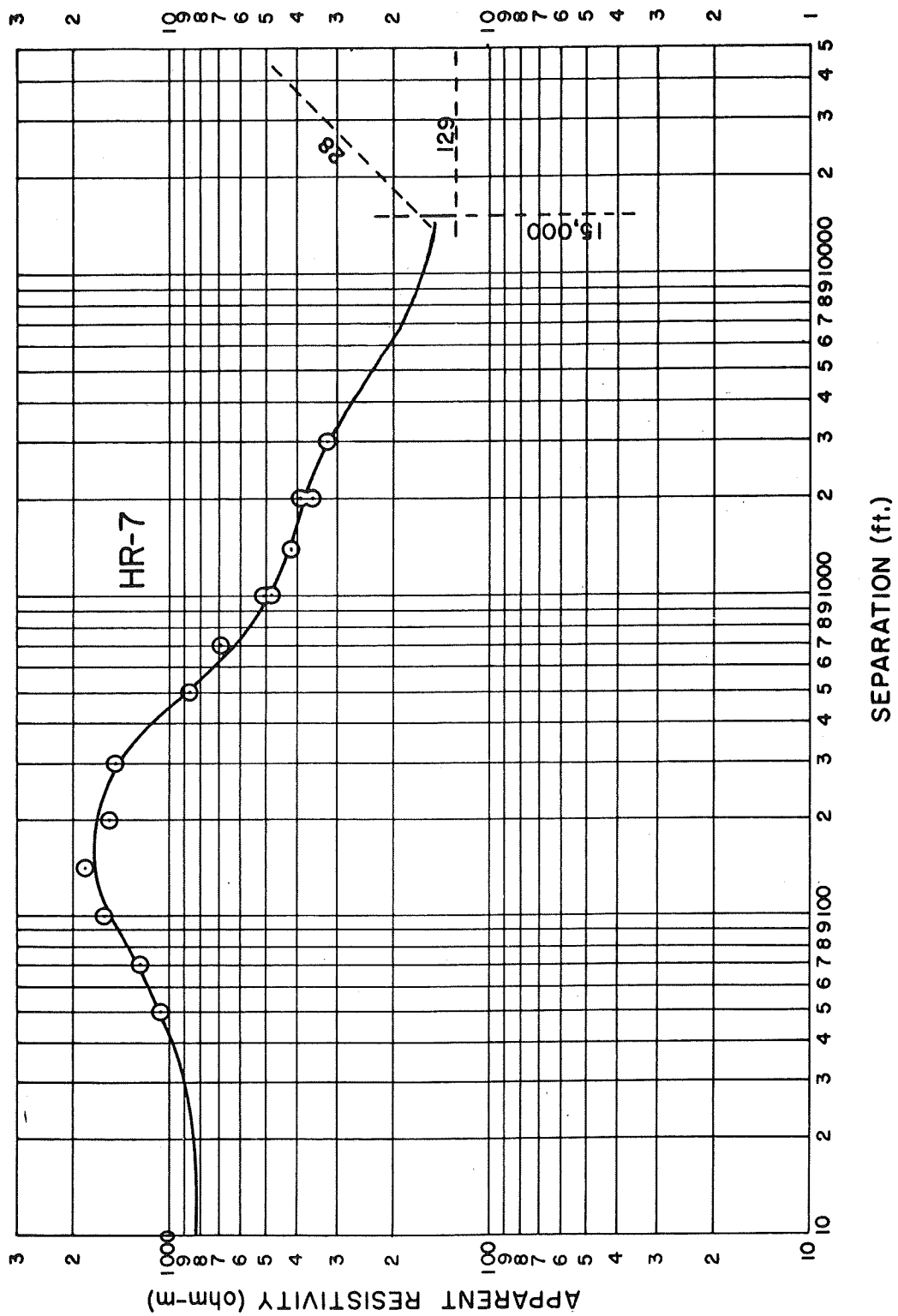
HR-7
88
129
15,000
APPARENT RESISTIVITY (ohm-m)
SEPARATION (ft.)

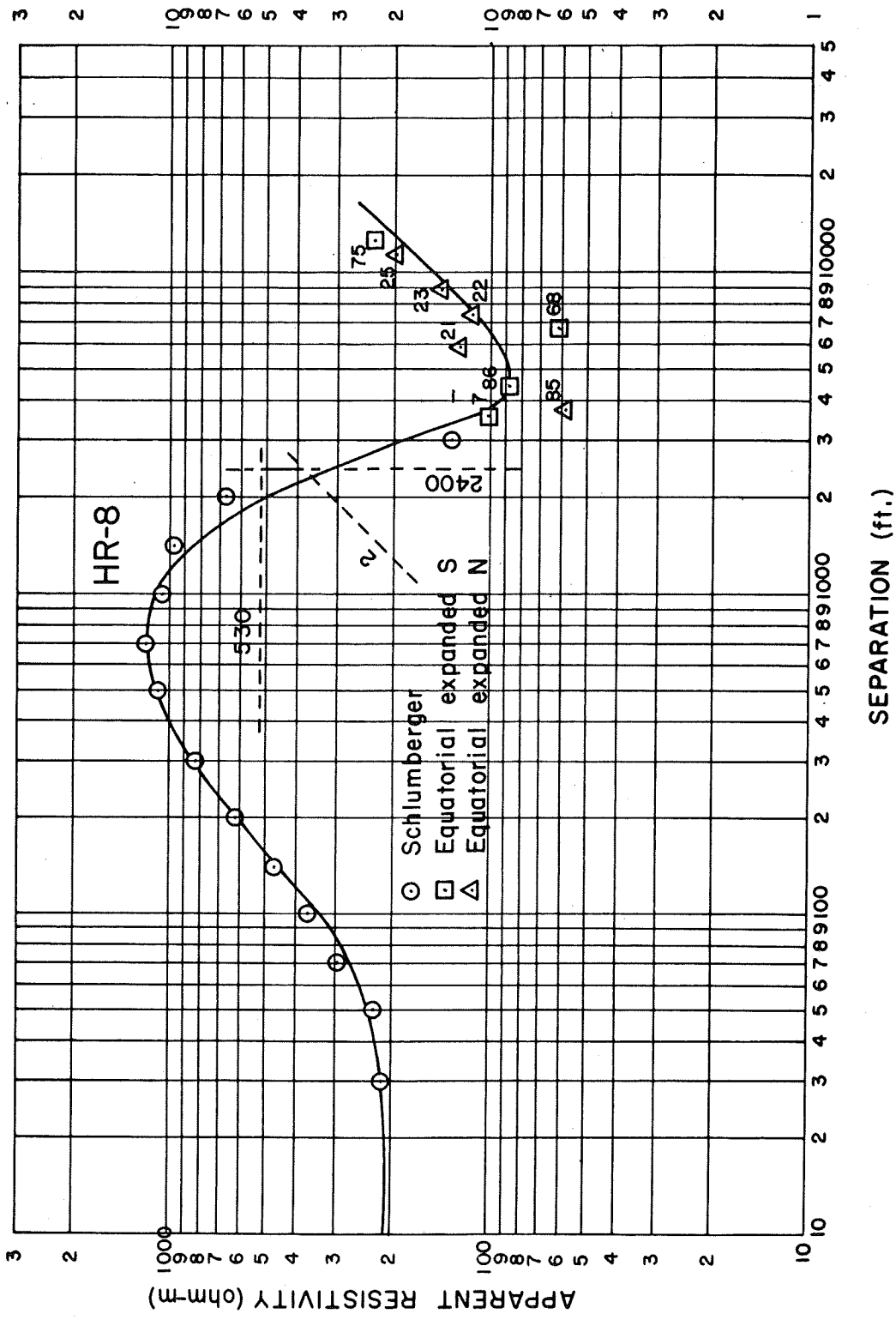
HR-8
530
2400
Schlumberger
Equatorial expanded S
Equatorial expanded N
APPARENT RESISTIVITY (ohm-m)
SEPARATION (ft.)

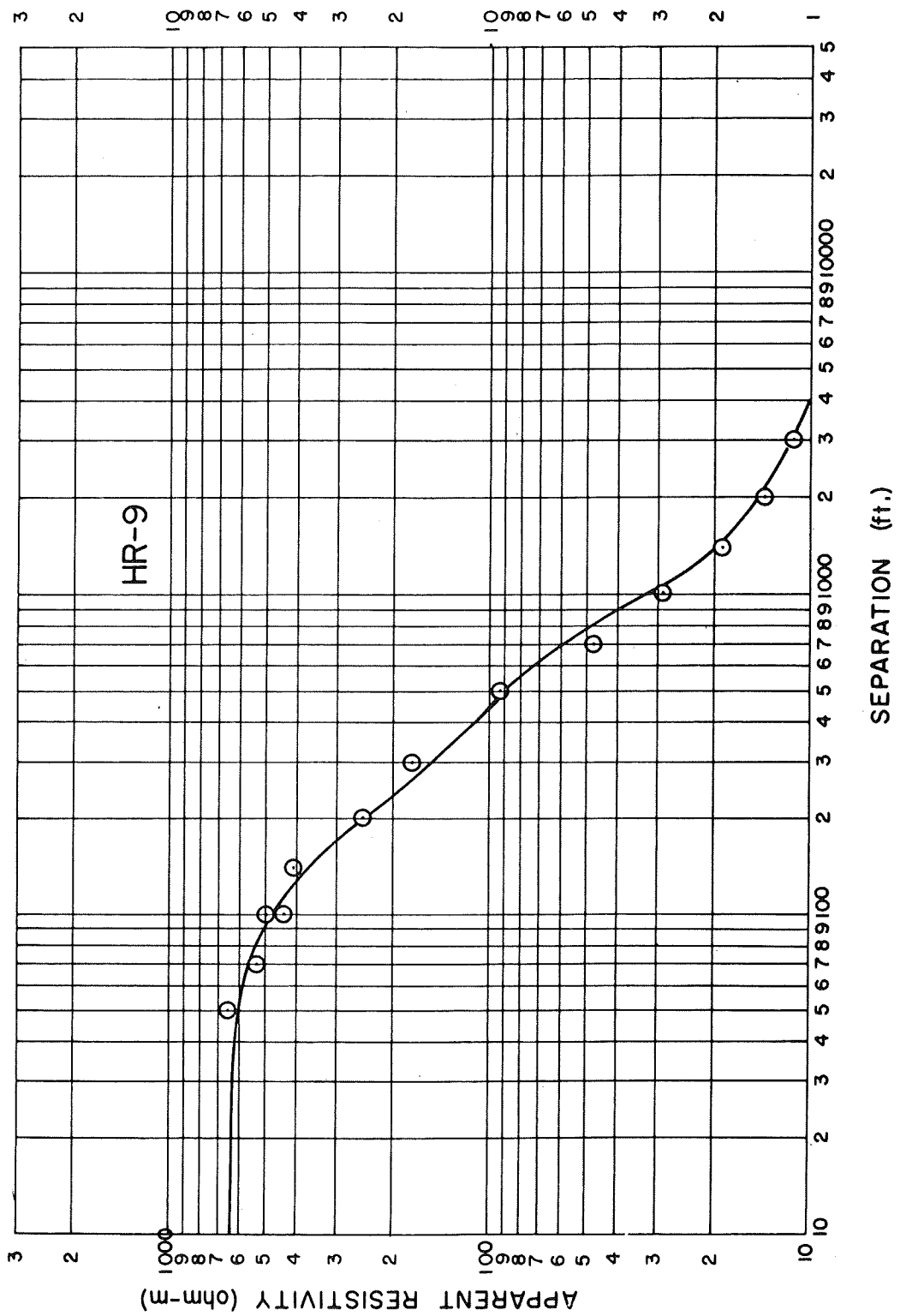
HR-9
APPARENT RESISTIVITY (ohm-m)
SEPARATION (ft.)

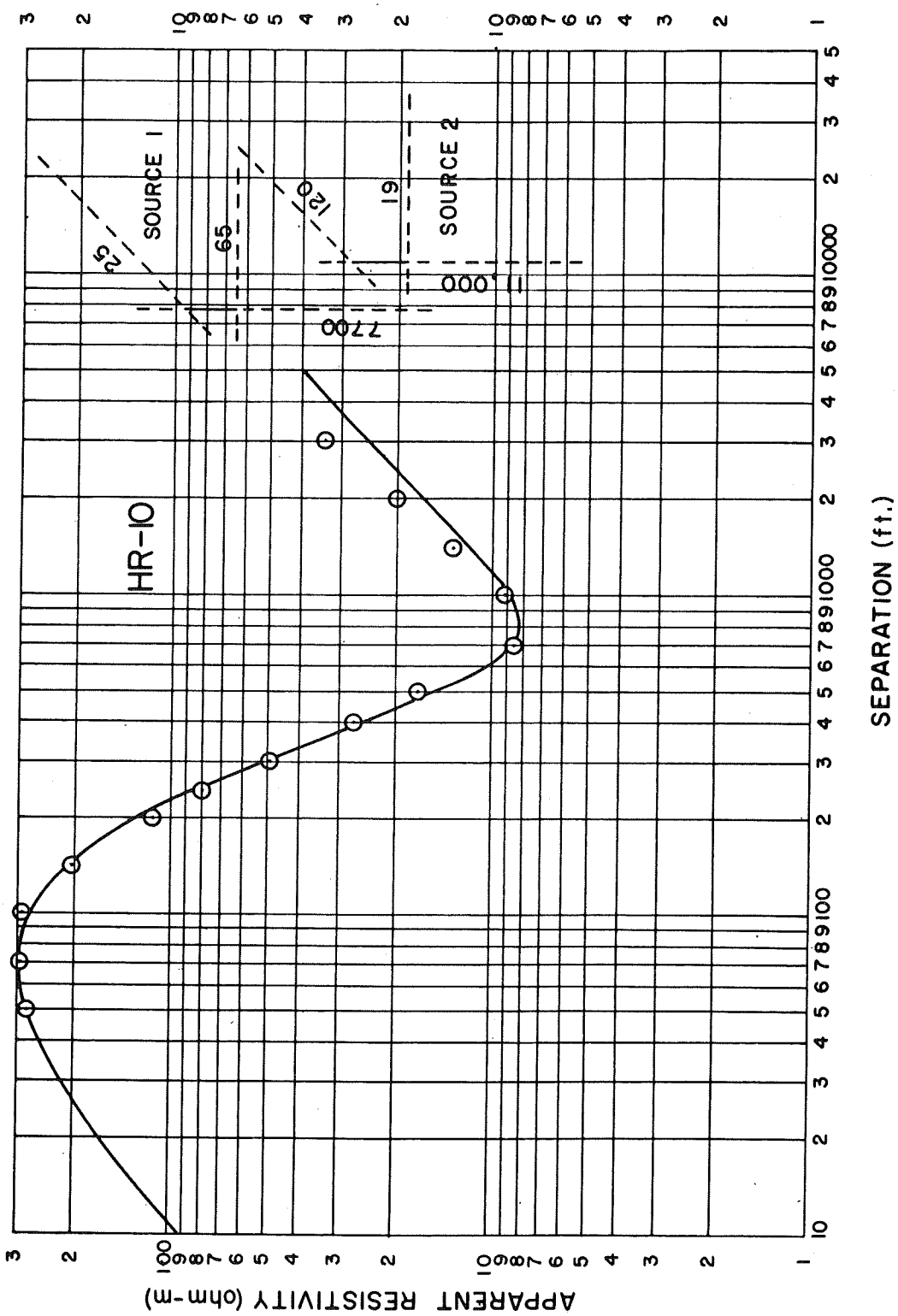
HR-10
SOURCE 1
SOURCE 2
65
22
12
19
7700
11,000
APPARENT RESISTIVITY (ohm-m)
SEPARATION (ft.)

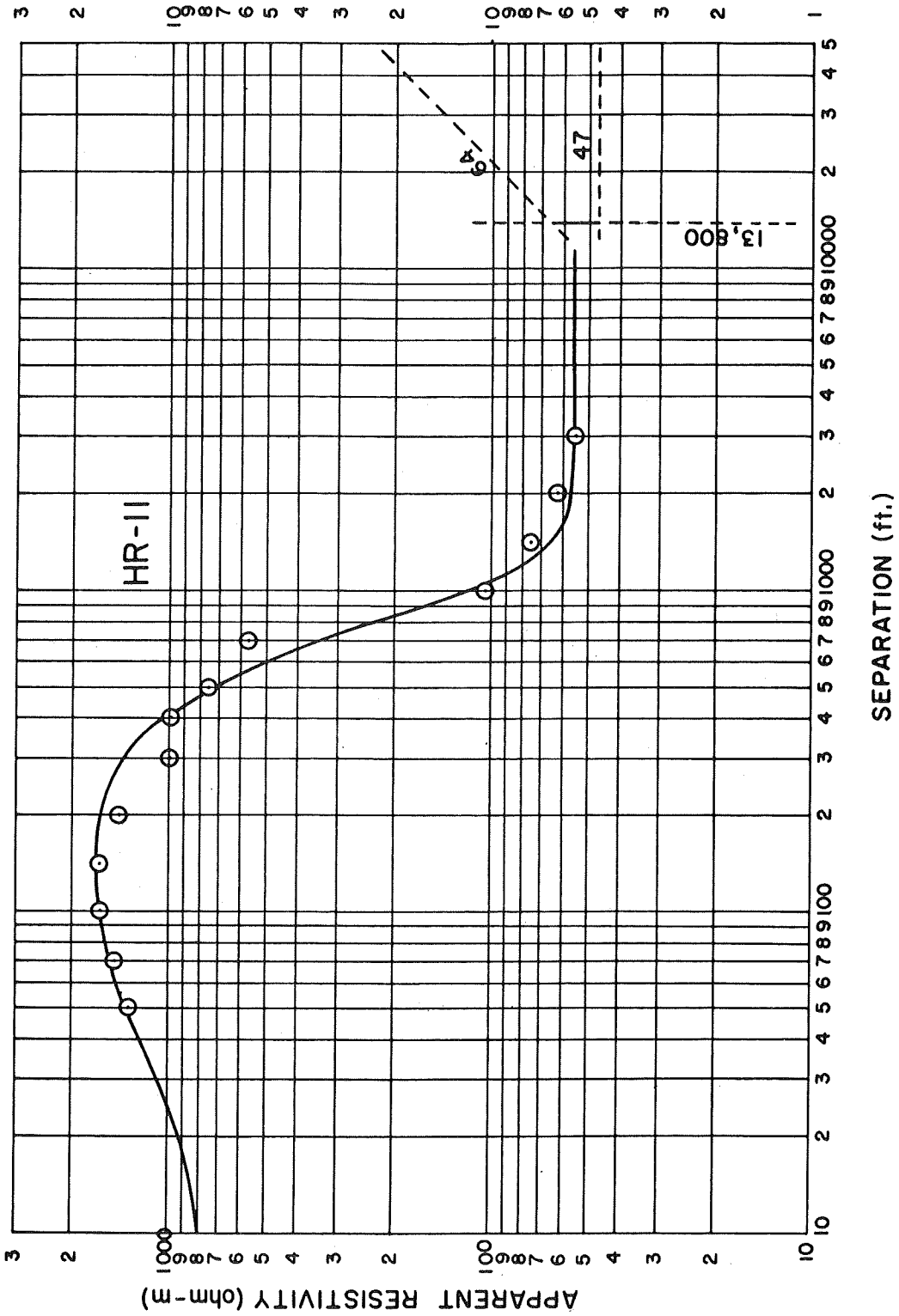
HR-11
13,600
47
APPARENT RESISTIVITY (ohm-m)
SEPARATION (ft.)

APPENDIX B

The following quantities for the dipole mapping survey are listed:

N	Station number
R1	Distance from observation point to one end of the source dipole, measured in miles
R2	Distance from observation point to the other end of the dipole source, measured in miles
D	The angle between the two lines R1 and R2 running from an observation point to the two ends of the source dipole
T	The angle between the two directions in which electric field measurements were made at each site, nominally 90 degrees
V1	Voltage measured between one pair of receiver electrodes, in microvolts
V2	Voltage measured between the other pair of receiver electrodes, in microvolts
L	Length of receiver dipole, in meters
I	Amplitude of current steps, in amperes
RA	Apparent resistivity calculated assuming spherical spreading of current in a uniform earth, in ohm-m
SA	Apparent conductance calculated assuming cylindrical spreading of current in a uniform conducting plate, in mhos

Source 1

N	R1	R2	D	T	V1	V2	L	I	RA	SA
1	0.33	1.64	0.	92.	3100.	300.	30.	1.00	192.3	2.
2	0.67	1.97	0.	93.	1100.	260.	30.	1.15	273.8	3.
3	1.01	2.31	0.	94.	220.	90.	30.	1.25	133.3	8.
3	1.01	2.31	0.	94.	360.	170.	30.	2.40	116.6	10.
4	1.33	2.63	0.	84.	180.	0.	30.	2.40	97.2	15.
5	1.71	3.02	0.	89.	400.	0.	91.	2.45	125.6	14.
6	2.09	3.39	0.	90.	200.	0.	91.	2.50	100.8	21.
7	0.66	0.68	166.	90.	2500.	8.	30.	3.05	100.5	11.
7	0.66	0.68	166.	90.	2200.	0.	30.	2.50	107.8	10.
8	0.34	1.65	0.	88.	5800.	600.	30.	2.53	150.4	3.
9	0.78	2.10	0.	89.	140.	30.	30.	2.56	21.3	43.
10	1.00	2.30	0.	87.	340.	110.	90.	2.60	30.2	37.
11	1.36	2.65	0.	104.	360.	40.	90.	2.60	66.8	22.
12	1.73	3.02	0.	85.	150.	90.	90.	2.60	52.2	34.
13	2.10	3.36	0.	110.	260.	220.	90.	3.00	182.3	11.
14	2.43	3.70	0.	94.	130.	50.	90.	3.10	86.4	27.
15	2.75	3.97	0.	86.	90.	0.	90.	3.10	76.5	34.
16	3.07	4.30	0.	87.	40.	0.	90.	3.30	42.2	68.
17	0.85	1.80	45.	98.	270.	40.	30.	3.10	41.4	29.
18	1.15	1.80	48.	89.	150.	40.	30.	3.10	45.4	38.
19	0.46	0.86	168.	90.	18000.	7500.	30.	3.30	528.6	2.
20	0.82	0.96	94.	92.	380.	620.	30.	3.05	69.1	20.
21	1.09	1.14	73.	92.	220.	620.	30.	3.01	124.9	14.
22	1.38	1.42	56.	88.	90.	290.	30.	3.04	111.9	20.
23	1.67	1.70	46.	88.	210.	640.	90.	3.06	143.1	19.

Source 1

N	R1	R2	D	T	V1	V2	L	I	RA	SA
24	1.91	2.00	39.	90.	420.	300.	90.	3.06	172.8	18.
25	2.09	2.17	36.	88.	440.	110.	90.	3.06	193.9	18.
26	2.16	2.33	34.	94.	40.	460.	90.	3.06	229.4	15.
27	2.52	2.61	29.	117.	310.	120.	90.	3.06	327.1	13.
28	0.74	1.32	73.	109.	70.	830.	30.	3.27	85.8	14.
29	0.88	1.19	71.	80.	400.	170.	30.	3.08	58.0	26.
30	1.06	1.50	58.	91.	200.	220.	30.	3.07	70.1	25.
31	0.92	2.20	7.	98.	550.	0.	90.	3.06	33.6	31.
32	1.02	2.23	17.	90.	600.	350.	90.	3.05	53.3	22.
33	1.33	2.47	20.	93.	280.	0.	90.	3.04	40.2	38.
34	1.68	2.82	17.	104.	170.	180.	90.	3.30	65.6	29.
35	1.94	3.14	12.	98.	120.	0.	90.	3.02	43.2	48.
36	2.40	3.61	10.	106.	110.	0.	90.	3.02	69.1	36.
37	2.74	3.97	9.	101.	90.	100.	90.	3.06	123.7	22.
38	2.90	4.17	6.	94.	140.	0.	90.	3.06	133.6	21.
39	3.18	4.46	5.	99.	110.	40.	90.	3.06	149.6	20.
40	1.41	2.71	0.	92.	330.	0.	90.	3.07	53.0	28.
41	1.41	2.71	0.	81.	110.	0.	90.	3.07	17.9	83.
43	1.56	2.57	24.	91.	140.	130.	90.	3.04	40.9	46.
44	1.61	2.46	30.	95.	160.	160.	90.	3.04	54.9	39.
45	1.64	2.31	34.	94.	300.	60.	90.	3.04	76.8	30.
46	1.91	2.78	24.	93.	150.	0.	90.	3.04	54.3	44.
47	2.26	3.07	23.	107.	80.	120.	90.	3.04	94.7	30.
48	2.53	3.40	20.	94.	70.	0.	90.	3.04	51.8	60.
49	2.61	3.57	17.	89.	60.	0.	90.	3.04	47.4	64.
50	2.70	3.76	14.	92.	80.	0.	90.	3.04	67.4	44.

Source 1

N	R1	R2	D	T	V1	V2	L	I	RA	SA
51	0.74	1.44	64.	96.	600.	460.	30.	3.17	81.5	14.
52	2.15	2.48	32.	94.	220.	200.	90.	3.17	150.8	23.
53	2.06	2.57	30.	90.	240.	100.	90.	3.17	114.8	27.
54	2.10	2.78	27.	94.	110.	140.	90.	3.17	83.4	35.
56	1.34	2.16	35.	80.	130.	350.	90.	3.18	50.6	36.
57	0.84	1.67	50.	97.	60.	340.	90.	3.18	16.6	74.
58	1.20	1.86	45.	100.	510.	390.	90.	3.18	75.3	24.
59	1.36	1.77	47.	93.	950.	0.	90.	3.18	135.8	16.
60	1.62	2.10	39.	94.	70.	310.	90.	3.18	73.6	34.
61	2.87	3.98	12.	92.	70.	0.	90.	3.04	68.2	45.
62	0.95	2.17	18.	112.	48.	0.	90.	3.17	3.2	344.
63	0.96	2.05	29.	86.	390.	450.	90.	3.17	37.1	32.
64	1.31	2.40	24.	90.	70.	80.	90.	3.17	14.1	111.
65	1.66	2.73	20.	92.	222.	50.	90.	3.17	54.2	35.
66	0.51	1.81	0.	95.	110.	810.	90.	3.17	13.4	48.
67	1.16	1.50	58.	131.	1100.	480.	90.	3.18	173.4	11.
68	1.24	1.33	61.	82.	440.	410.	30.	3.18	154.7	13.
69	1.04	1.28	68.	89.	270.	70.	30.	3.18	52.8	33.
70	1.78	3.07	5.	87.	240.	80.	90.	3.32	64.5	28.
71	2.13	3.41	5.	89.	110.	0.	90.	3.28	44.9	48.
72	2.49	3.77	4.	94.	190.	0.	90.	3.28	115.0	21.
73	2.82	4.11	3.	90.	60.	0.	90.	3.27	49.7	55.
74	1.92	2.11	38.	106.	540.	300.	90.	3.27	235.6	13.
75	2.26	2.32	34.	91.	230.	390.	90.	3.27	225.3	16.
76	2.58	2.59	30.	95.	230.	310.	90.	3.27	287.8	14.
77	2.85	2.95	26.	92.	190.	0.	90.	3.27	194.4	24.

Source 1

N	R1	R2	D	T	V1	V2	L	I	RA	SA
78	3.13	3.29	24.	93.	150.	0.	90.	3.27	200.2	25.
79	3.42	3.62	21.	90.	130.	0.	90.	3.27	233.3	23.
80	3.69	3.92	20.	94.	120.	0.	90.	3.27	261.8	22.
81	3.99	4.25	19.	88.	60.	0.	90.	3.27	159.4	40.
82	0.87	1.66	52.	113.	190.	510.	30.	3.27	96.6	13.
83	1.98	3.04	18.	88.	250.	0.	90.	3.30	88.0	26.
84	2.33	3.36	17.	91.	110.	50.	90.	3.30	64.7	41.
85	0.67	0.73	138.	93.	1300.	370.	30.	3.30	58.8	19.
86	0.84	0.86	113.	85.	700.	910.	30.	3.30	78.4	17.
87	2.39	2.61	30.	96.	320.	110.	90.	3.45	209.8	18.
88	2.24	2.66	30.	89.	270.	160.	90.	3.42	157.6	22.
89	2.16	2.77	28.	93.	140.	210.	90.	3.40	117.9	26.
90	2.13	2.90	25.	95.	130.	300.	90.	3.38	146.6	19.
91	2.19	3.11	21.	95.	0.	250.	90.	3.38	113.8	23.
92	2.10	3.17	17.	90.	0.	230.	90.	3.39	91.0	26.
93	2.15	3.31	14.	91.	130.	160.	90.	3.40	85.1	27.
93	2.15	3.31	14.	91.	0.	240.	90.	3.47	96.4	24.
94	2.38	3.67	5.	86.	0.	260.	90.	3.51	130.6	18.
95	2.26	3.50	9.	87.	110.	290.	90.	3.49	136.3	17.
96	2.78	2.88	27.	91.	280.	140.	90.	3.42	282.6	16.
98	2.31	3.00	25.	90.	210.	0.	90.	3.59	107.3	29.
99	2.50	3.07	25.	94.	120.	90.	90.	3.57	100.7	35.
100	2.63	3.27	25.	84.	120.	110.	90.	3.55	110.0	34.
101	2.13	2.67	29.	88.	220.	150.	90.	3.55	112.0	28.
102	2.48	3.01	26.	94.	60.	190.	90.	3.50	131.9	27.
103	2.69	3.33	22.	90.	110.	110.	90.	3.50	125.0	29.

Source 1

N	R1	R2	D	T	V1	V2	L	I	RA	SA
104	2.83	3.57	20.	83.	80.	80.	90.	3.50	95.5	38.
105	1.98	2.30	35.	100.	470.	50.	90.	3.60	166.2	19.
106	1.93	2.47	32.	89.	380.	110.	90.	3.60	126.8	23.
107	1.88	2.63	28.	91.	240.	260.	90.	3.59	105.9	24.
108	1.14	2.07	35.	91.	30.	800.	30.	3.57	205.0	7.
109	1.45	2.44	26.	91.	290.	60.	30.	3.57	135.5	13.
110	1.71	2.66	25.	96.	150.	50.	30.	3.55	112.6	19.
111	2.15	3.05	22.	88.	220.	50.	90.	3.54	92.7	28.
112	2.51	3.38	19.	93.	170.	60.	90.	3.54	115.4	26.
113	2.87	3.64	19.	89.	140.	0.	90.	3.52	129.0	28.
114	3.08	3.80	19.	109.	130.	60.	90.	3.51	189.6	21.
115	3.35	3.93	19.	91.	100.	0.	90.	3.52	147.0	32.
116	2.38	2.61	30.	95.	50.	120.	30.	3.51	234.8	16.
117	2.75	2.97	27.	93.	60.	120.	90.	3.49	118.0	38.
118	2.85	3.25	24.	89.	250.	60.	90.	3.46	251.9	17.
119	3.09	3.58	21.	111.	50.	150.	90.	3.46	229.6	20.
120	3.40	4.42	14.	104.	0.	120.	90.	3.49	164.7	23.
121	3.36	4.40	12.	93.	90.	80.	90.	3.50	161.3	22.
122	3.00	4.19	9.	93.	0.	90.	90.	3.51	83.5	36.

Source 2

N	R1	R2	D	T	V1	V2	L	I	RA	SA
151	0.59	1.31	59.	97.	200.	300.	30.	8.10	9.8	91.
152	0.97	1.67	40.	34.	70.	170.	30.	8.10	14.5	93.
153	1.19	1.97	30.	100.	0.	500.	90.	8.10	22.7	67.
154	1.47	2.32	23.	99.	260.	500.	90.	8.10	44.9	39.
155	1.32	2.72	17.	99.	60.	160.	90.	8.15	22.7	90.
156	2.13	3.03	15.	92.	90.	30.	90.	8.15	19.0	127.
157	2.53	3.42	14.	92.	50.	30.	90.	8.15	17.2	162.
158	2.73	3.70	11.	93.	40.	20.	90.	8.15	17.1	171.
159	3.21	4.09	11.	87.	20.	0.	90.	8.17	11.1	310.
160	0.39	1.32	52.	92.	1000.	240.	30.	8.18	11.0	51.
161	1.16	1.50	43.	92.	150.	50.	30.	8.10	19.3	97.
163	1.32	1.43	43.	96.	160.	0.	30.	8.10	24.5	89.
164	1.45	1.79	39.	106.	90.	220.	90.	8.10	19.8	116.
165	1.77	2.17	31.	100.	80.	170.	90.	8.10	25.3	104.
166	2.07	2.56	25.	105.	120.	150.	90.	8.15	42.9	68.
167	2.36	2.91	22.	93.	0.	90.	90.	8.15	24.1	134.
168	2.72	3.31	19.	97.	0.	90.	90.	8.15	35.2	102.
169	3.10	3.67	17.	92.	0.	60.	90.	8.15	33.7	122.
170	3.51	4.07	15.	77.	0.	60.	90.	8.15	49.4	93.
171	0.71	1.72	25.	37.	40.	300.	30.	8.20	11.8	74.
172	1.12	2.17	14.	99.	420.	240.	90.	8.20	19.3	64.
173	1.47	2.46	16.	90.	320.	40.	90.	8.70	21.8	75.
174	1.33	2.32	15.	82.	30.	20.	90.	8.50	10.4	198.
175	2.17	3.02	16.	94.	100.	0.	90.	8.70	18.7	131.
176	0.61	0.76	103.	35.	250.	340.	30.	8.70	14.8	72.

Source 2

N	R1	R2	D	T	V1	V2	L	I	RA	SA
177	0.67	1.02	102.	90.	740.	1400.	30.	8.70	37.9	32.
178	0.97	2.03	5.	93.	420.	360.	90.	9.00	13.7	78.
179	1.00	2.10	3.	99.	240.	320.	90.	9.00	11.3	97.
180	1.18	2.03	24.	89.	160.	210.	90.	9.05	10.1	139.
181	3.92	4.46	14.	93.	0.	60.	90.	8.20	65.2	80.
182	1.51	2.03	32.	97.	110.	380.	90.	8.20	33.3	64.
183	1.58	2.33	25.	95.	240.	0.	90.	8.20	21.6	92.
184	1.78	2.62	20.	90.	90.	170.	90.	8.20	22.8	92.
185	1.96	2.83	15.	90.	90.	110.	90.	8.50	20.5	105.
186	2.46	3.23	14.	90.	70.	50.	90.	8.50	23.3	117.
187	2.49	3.48	10.	90.	90.	0.	90.	8.50	23.6	108.
188	3.17	4.16	8.	97.	50.	40.	90.	8.70	32.9	96.
189	0.38	1.50	0.	98.	6400.	2700.	30.	8.95	63.7	7.
190	0.68	1.79	11.	104.	410.	190.	30.	9.00	16.4	49.
191	0.99	2.10	4.	115.	90.	100.	30.	9.00	13.4	81.
192	1.53	2.65	0.	110.	300.	150.	90.	9.00	23.3	55.
193	1.95	3.06	2.	92.	90.	110.	90.	9.00	18.6	104.
194	2.34	3.44	4.	95.	150.	60.	90.	9.00	34.0	67.
195	2.70	3.81	3.	102.	0.	70.	90.	9.00	21.0	122.
196	3.05	4.14	4.	90.	90.	0.	90.	9.00	36.5	79.
197	3.42	4.51	4.	90.	70.	50.	90.	9.00	47.1	68.
198	1.48	1.51	40.	95.	140.	460.	90.	9.60	30.4	79.
199	1.72	2.73	10.	96.	210.	130.	90.	9.60	23.0	78.
200	1.90	3.00	5.	105.	0.	160.	90.	9.60	18.7	101.
201	1.23	2.02	30.	89.	260.	220.	90.	9.00	16.3	102.
202	2.23	3.35	3.	89.	70.	110.	90.	9.60	21.7	100.

Source 2

N	R1	R2	D	T	V1	V2	L	I	RA	SA
203	2.34	3.47	0.	96.	0.	80.	90.	9.80	14.9	151.
204	2.52	3.63	4.	113.	0.	50.	90.	9.75	12.3	198.
205	1.50	2.61	3.	94.	80.	0.	90.	9.75	5.0	308.
206	1.68	2.80	2.	105.	170.	50.	90.	9.75	16.0	106.
207	1.36	2.96	5.	90.	80.	80.	90.	9.75	11.9	156.
208	0.23	1.27	47.	96.	11000.	33000.	30.	10.00	105.6	3.
209	0.62	1.48	44.	84.	630.	180.	30.	9.95	16.3	52.
210	0.83	1.72	33.	100.	240.	80.	30.	9.90	12.5	85.
211	0.70	1.26	62.	86.	610.	50.	30.	9.90	18.3	61.
212	1.03	1.48	49.	89.	120.	90.	30.	9.90	12.4	139.
213	2.21	3.21	11.	88.	160.	0.	90.	9.85	26.5	87.
214	1.95	2.99	10.	92.	140.	0.	90.	9.85	16.7	120.
215	1.70	2.78	8.	95.	220.	80.	90.	9.85	20.2	86.
216	1.55	2.66	6.	80.	50.	200.	90.	9.85	13.3	120.

REFERENCES

1. Frazer, H. J., Wilson, H. B. D., and Hendry, N. W., 1943, Hot Springs Deposits of the Coso Mountains: Calif. Jour. Mines Geol., v. 38, pp. 223-42.

2. Ross, Clyde P., and Yates, Robert G., 1943, The Coso Quicksilver District, Inyo County, California. U. S. Geol. Surv. Bull. 936-Q, pp. 395-416.

3. Chesterman, C. W., 1956, Pumice, Pumicite, and Volcanic Cinders in California. Calif. Div. Mines Bull. 174.

4. Austin, Carl F., 1964, Coso Hot Springs - A Geologic Challenge. U. S. Naval Ordnance Test Station, China Lake, California, NOTS TS 64-180.

5. Koenig, J. B., Gawarecki, S. L., and Austin, C. A., 1972, Remote Sensing of the Coso Geothermal Area, Inyo County, California. U. S. Naval Weapons Center, China Lake, California, Technical Paper 5233.

6. Jennings, C. W., 1958, Geologic Map of California, Death Valley Sheet. California Div. Mines Geol.

7. Moyle, W. R., Jr., 1963, Water Wells of Indian Wells Valley, California. Calif. Department of Water Resources, Bulletin 91-9.

8. Schultz, J. R., 1937, A late Cenozoic Vertebrate Fauna From the Coso Mountains, Inyo County, California. Carnegie Inst., Washington Pub., No. 487.

9. Austin, Carl F., Austin, Ward H., and Leonard, G. W., 1971, Geothermal Science and Technology - A National Program. Naval Weapons Center, China Lake, California, Technical Series 45-029-72.

10. Hall, W. E., and MacKevett, E. M., 1962, Geology and Ore Deposits of the Darwin Quadrangle, Inyo County, California. U. S. Geol. Survey Prof. Paper 368.

11. Austin, C. F., and Pringle, J. K., 1970, Geologic Investigations at the Coso Thermal Area. Naval Weapons Center, China Lake, California, NWC TP 4878.

12. Dupuy, Leon W., 1948, Bucket-Drilling the Coso Mercury Deposit, Inyo County, California. U. S. Bureau Mines, Rept. Invest. 4201, 45 p.

13. Banwell, C. J., 1970, Geophysical Techniques in Geothermal Exploration. Section IV, United Nations Symposium on the Development and Utilization of Geothermal Resources, Pisa, Italy.

14. Furgerson, Robert B., 1970, A Controlled-Source Telluric Current Technique and Its Application to Structural Investigations. Unpublished M.S. Thesis T-1313, Colorado School of Mines.

15. Chastenet de Gery, Jerome, and Kunetz, Geza, 1956, Potential and Apparent Resistivity Over Dipping Beds. Geophysics, v. 21, pp. 780-793.

16. Keller, G. V., and Frsichknecht, F. C., 1966, Electrical Methods in Geophysical Prospecting. Pergamon Press, New York.

17. Stacey, F. D., 1969, Physics of the Earth. Wiley, New York, 324 p.

18. Meidav, Tsvi, and Furgerson, R. B., 1972, Resistivity Studies of the Imperial Valley Geothermal Area, California. Geothermics, v. 1, no. 2, pp. 46-62.

19. Healy, J. H. and Press, Frank, 1964, Geophysical Studies of Basin Structures Along the Eastern Front of the Sierra Nevada, California. Geophysics, v. 29, no. 3, pp. 337-359.

20. Zohdy, Adel, 1965, The Auxiliary Point Method of Electrical Sounding and Its Relationship to the Dar Zarrouk Parameters. Geophysics, v. 30, no. 4, pp. 644-660.

21. Orellana, E., and Mooney, H. M., 1966, Master Tables and Curves for Vertical Electrical Sounding Over Layered Structures. Madrid, Interciencia.

22. Crous, C. M., 1971, Computer-Assisted Interpretation of Electrical Soundings. M.Sc. Thesis T-1363, Colorado School of Mines.

23. Argelo, S. M., 1967, Two Computer Programs for the Calculation of Standard Graphs for Resistivity Prospecting. Geophysical Prospecting, v. 15, no. 1, pp. 71-92.

24. Alpin, L. M, 1966, The Theory of Dipole Sounding in Dipole Methods for Measuring Earth Conductivity. Consultant's Bureau, New York, 302 p.

25. Furgerson, Robert, and Keller, George, 1973, Catalogue of Dipole Mapping Curves. Office of Naval Research report in preparation.

26. Teledyne Geotech, 1972, Geothermal Noise Survey of the Coso Hot Springs Area. Naval Weapons Center, China Lake, California, unpublished Technical Report No. 72-6 produced under contract by Teledyne Geotech for the Naval Weapons Center, China Lake, California.

27. Zohdy, Adel, and Jackson, Dallas, 1969, Application of Deep Electrical Soundings for Groundwater Exploration in Hawaii. Geophysics, v. 34, no. 4., pp. 584-600.

28. Berdichevskii, M. N., and Petrovskii, A. D., 1956, Methods of Bilateral Equatorial Sounding. Prikladnaya Geofiziki, v. 14, pp. 97-114 (in Russian).

1 Central Intelligence Agency, Langley Air Force Base
11 Coast and Geodetic Survey
Marine Geology Unit (1)
Dr. D. F. Peck (1)
William F. Fisher (1)
Joules D. Friedman (1)
Steven Gowarecki (1)
William R. Hemphill (1)
V. E. McKelvy (1)
William A. Radlinski (1)
Edwin Roedder (1)
Reed Stone (1)
Russell G. Wayland (1)
Richard S. Williams (1)
1 Department of the Interior, Bureau of Reclamation (Assistant to the Commissioner for Geothermal Resources, Dr. Chung-Ming Wong)
1 National Aeronautics & Space Administration (Earth Observation Program, Earth Sciences Survey)
2 Goddard Space Flight Center
Paul D. Loman (1)
Nicolas Short (1)
2 National Science Foundation (Office of Intergovernmental Science Program, Harold Metcalf)
1 California Academy of Sciences, San Francisco, Calif. Department of Geology, Dr. Ian Campbell)
1 California Department of Conservation, Sacramento, Calif. (Lawrence H. Axtel)
3 California Department of Water Resources, Los Angeles, Calif.
Chief Planning Division (1)
Jack J. Coe (1)
Technical Library (1)
1 California Department of Water Resources, Sacramento, Calif. (Geology Staff Specialist, Raymond C. Richter)
2 California Division of Mines and Geology, Sacramento, Calif.
Associate Geophysicist, Roger H. Chapman (1)
J. B. Koenig (1)
4 California Division of Mines, San Francisco, Calif.
R. H. Chapman (1)
M. Stinson (1)
B. Troxel (1)
2 California Division of Oil and Gas, Sacramento, Calif.
David M. Anderson (1)
Marshall Reed (1)
5 Colorado School of Mines, Golden Colo.
Department of Geology
R. Epis (1)
L. T. Grose (1)
Department of Geological Engineering, Robert Reeves (1)
Department of Geophysics
Ralph Holmer (1)
George Keller (1)

List Continued on Inside Back Cover

INITIAL DISTRIBUTION

2 Naval Air Systems Command (AIR-50174)
1 Chief of Naval Material (MAT-03T1)
2 Naval Facilities Engineering Command
  FAC-03 (1)
  FAC-07 (1)
1 Naval Facilities Engineering Command, Western Division
2 Naval Ordnance Systems Command (ORD-0632)
1 Chief of Naval Research, Arlington
1 Naval Civil Engineering Laboratory, Port Hueneme (Sterling L. Bugg)
1 Naval Research Laboratory (Code 5230, Energy Conversion Branch)
1 Naval Scientific and Technical Intelligence Center, (W. T. Peterson)
3 Naval Undersea Center, San Diego
  Dr. W. B. McLean (1)
  George Wilkins (1)
1 Oceanographer of the Navy, Alexandria
1 Chief of Engineers (Bruce Hall)
1 Air Force Flight Test Center, Edwards Air Force Base, (Chief Scientist)
1 Director of Defense Research and Engineering (Research Advanced Technology, Capt. Gordon Smith)
1 Defense Advanced Research Projects Agency, Arlington (S. Ruby)
1 Defense Atomic Support Agency, Sandia Base (Technical Library)
1 Office of Science & Technology (Assistant Director of Energy and Environment, Dr. Richard Balzhiser)
12 Defense Documentation Center
2 Atomic Energy Commission (Division of Peaceful Nuclear Explosives)
  Director (1)
  A. H. Ewing (1)
1 Atomic Energy Commission, Las Vegas, Nev. (Director, Engineering and Construction Division)
1 Bureau of Land Management, Bakersfield, Calif. (Frederick S. Crafts)
2 Bureau of Land Management, Sacramento, Calif.
  State Director (1)
  Chief, Branch of Minerals (1)
1 Bureau of Mines, Arizona, University of Arizona, Tucson (Director)
1 Bureau of Mines, Idaho, Moscow, Idaho (Director)
2 Bureau of Mines, Nevada, University of Nevada, Reno, Nev. (John Schilling)
3 Bureau of Mines and Mineral Resources, New Mexico, Socorro, N. Mex.
  Director (1)
  Kelly Summers (1)
  Robert Weber (1)
2 Bureau of Mines
  Assistant Director for Minerals Research (1)
  Director, Mining Research (1)

UNCLASSIFIED
Security Classification

DOCUMENT CONTROL DATA - R & D

(Security classification of title, body of abstract and indexing annotation must be entered when the overall report is classified)

1. ORIGINATING ACTIVITY *(Corporate author)*
Naval Weapons Center
China Lake, California 93555

2a. REPORT SECURITY CLASSIFICATION
UNCLASSIFIED

2b. GROUP

3. REPORT TITLE
PROGRESS REPORT ON ELECTRICAL RESISTIVITY STUDIES, COSO GEOTHERMAL AREA, INYO COUNTY, CALIFORNIA

4. DESCRIPTIVE NOTES *(Type of report and inclusive dates)*
A progress report

5. AUTHOR(S) *(First name, middle initial, last name)*
Robert B. Furgerson

6. REPORT DATE	7a. TOTAL NO. OF PAGES	7b. NO. OF REFS
June 1973	66	28

8a. CONTRACT OR GRANT NO.	9a. ORIGINATOR'S REPORT NUMBER(S)
b. PROJECT NO.	NWC TP 5497
c. Discretionary funds	9b. OTHER REPORT NO(S) *(Any other numbers that may be assigned this report)*
d.	

10. DISTRIBUTION STATEMENT
Approved for public release; distribution unlimited.

11. SUPPLEMENTARY NOTES	12. SPONSORING MILITARY ACTIVITY
	Naval Weapons Center China Lake, California 93555

13. ABSTRACT

This report describes the first phase of an electrical geophysical survey being conducted in the vicinity of the Coso Hot Springs, California, and contains data obtained through June 1972. The Coso Geothermal Area has been selected as an area for investigation and evaluation of its potential for geothermal energy.

14. KEY WORDS	LINK A		LINK B		LINK C	
	ROLE	WT	ROLE	WT	ROLE	WT
Geothermal Energy Geophysical Survey Electrical Resistivity Survey						

ABSTRACT CARD

Naval Weapons Center

Progress Report on Electrical Resistivity Studies, Coso Geothermal Area, Inyo County, California, by Robert B. Furgerson. Colorado School of Mines. China Lake, Calif., NWC, June 1973, 66 pp. (NWC TP 5497, publication UNCLASSIFIED.)

ABSTRACT. This report describes the first phase of an electrical geophysical survey being conducted in the vicinity of the Coso Hot Springs, California, and contains data obtained through June 1972. The Coso Geothermal Area has been selected as an area for investigation and evaluation of its potential for geothermal energy.

1 card, 8 copies

Naval Weapons Center

Progress Report on Electrical Resistivity Studies, Coso Geothermal Area, Inyo County, California, by Robert B. Furgerson. Colorado School of Mines. China Lake, Calif., NWC, June 1973, 66 pp. (NWC TP 5497, publication UNCLASSIFIED.)

ABSTRACT. This report describes the first phase of an electrical geophysical survey being conducted in the vicinity of the Coso Hot Springs, California, and contains data obtained through June 1972. The Coso Geothermal Area has been selected as an area for investigation and evaluation of its potential for geothermal energy.

1 card, 8 copies

Naval Weapons Center

Progress Report on Electrical Resistivity Studies, Coso Geothermal Area, Inyo County, California, by Robert B. Furgerson. Colorado School of Mines. China Lake, Calif., NWC, June 1973, 66 pp. (NWC TP 5497, publication UNCLASSIFIED.)

ABSTRACT. This report describes the first phase of an electrical geophysical survey being conducted in the vicinity of the Coso Hot Springs, California, and contains data obtained through June 1972. The Coso Geothermal Area has been selected as an area for investigation and evaluation of its potential for geothermal energy.

1 card, 8 copies

Naval Weapons Center

Progress Report on Electrical Resistivity Studies, Coso Geothermal Area, Inyo County, California, by Robert B. Furgerson. Colorado School of Mines. China Lake, Calif., NWC, June 1973, 66 pp. (NWC TP 5497, publication UNCLASSIFIED.)

ABSTRACT. This report describes the first phase of an electrical geophysical survey being conducted in the vicinity of the Coso Hot Springs, California, and contains data obtained through June 1972. The Coso Geothermal Area has been selected as an area for investigation and evaluation of its potential for geothermal energy.

1 card, 8 copies

ABSTRACT CARD

Naval Weapons Center

Progress Report on Electrical Resistivity Studies, Coso Geothermal Area, Inyo County, California, by Robert B. Furgerson. Colorado School of Mines. China Lake, Calif., NWC, June 1973, 66 pp. (NWC TP 5497, publication UNCLASSIFIED.)

ABSTRACT. This report describes the first phase of an electrical geophysical survey being conducted in the vicinity of the Coso Hot Springs, California, and contains data obtained through June 1972. The Coso Geothermal Area has been selected as an area for investigation and evaluation of its potential for geothermal energy.

1 card, 8 copies

Naval Weapons Center

Progress Report on Electrical Resistivity Studies, Coso Geothermal Area, Inyo County, California, by Robert B. Furgerson. Colorado School of Mines. China Lake, Calif., NWC, June 1973, 66 pp. (NWC TP 5497, publication UNCLASSIFIED.)

ABSTRACT. This report describes the first phase of an electrical geophysical survey being conducted in the vicinity of the Coso Hot Springs, California, and contains data obtained through June 1972. The Coso Geothermal Area has been selected as an area for investigation and evaluation of its potential for geothermal energy.

1 card, 8 copies

Naval Weapons Center

Progress Report on Electrical Resistivity Studies, Coso Geothermal Area, Inyo County, California, by Robert B. Furgerson. Colorado School of Mines. China Lake, Calif., NWC, June 1973, 66 pp. (NWC TP 5497, publication UNCLASSIFIED.)

ABSTRACT. This report describes the first phase of an electrical geophysical survey being conducted in the vicinity of the Coso Hot Springs, California, and contains data obtained through June 1972. The Coso Geothermal Area has been selected as an area for investigation and evaluation of its potential for geothermal energy.

1 card, 8 copies

Naval Weapons Center

Progress Report on Electrical Resistivity Studies, Coso Geothermal Area, Inyo County, California, by Robert B. Furgerson. Colorado School of Mines. China Lake, Calif., NWC, June 1973, 66 pp. (NWC TP 5497, publication UNCLASSIFIED.)

ABSTRACT. This report describes the first phase of an electrical geophysical survey being conducted in the vicinity of the Coso Hot Springs, California, and contains data obtained through June 1972. The Coso Geothermal Area has been selected as an area for investigation and evaluation of its potential for geothermal energy.

1 card, 8 copies

1 Federal Power Commission (Division of Electrical Resources and Requirements, Bureau of Power, Bernard B. Chew)
1 Geological Consultant, Klamath Falls, Ore. (Eugene V. Giancanelli)
1 Geological Consultant, Phoenix, Ariz. (Grischom Clacey)
6 Geological Survey, Denver, Colo.
  Gorden Eston (1)
  Leonard Gard (1)
  Don R. Mabey (1)
  Howard Waldren (1)
  Adel Zohdy (1)
  C. J. Zablocki (1)
1 Geological Survey, Garden Grove, Calif. (Ground Water Branch, W. R. Movle, Jr.)
1 Geological Survey, Los Angeles, Calif. (Oil and Gas Branch, John Fackler)
5 Geological Survey, Menlo Park, Calif.
  Roland von Huene (1)
  Gene Rusnak (1)
  G. I. Smith (1)
  Park Snavely (1)
  Donald E. White (1)
2 Los Angeles Department of Water and Power, Los Angeles
  John W. Arlidge (1)
  Howard R. King (1)
1 Office of Peaceful Nuclear Explosives, Nevada Operations Office, Las Vegas (D. W. Sherwood)
1 State Department of Water Resources, Sacramento, Calif. (R. C. Richter)
1 Washington Division of Mines and Geology, Olympia, Wash.
1 American Thermal Resources, Bakersfield, Calif. (Roy Parodi)
1 Battelle Memorial Institute, Pacific Northwest Laboratory (D. H. Stewart)
2 California Institute of Technology, Pasadena
  Prof. Leon T. Silver (1)
  Technical Library (1)
1 Brigham Young University, Provo, Utah (Director Economic Development, Clyde Davis)
1 Cheveron Oil Field Research Co., La Habra, Calif. (S. Yungel)
1 Coastal States Gas Producing Company, Corpus Christi, Tex. (J. A. Short)
1 Cornell University, Ithaca, N. Y. (Department of Geology, George A. Kieisch)
2 Department of Geology and Mineral Industries, Portland, Ore.
  Director (1)
  H. M. Dole (1)
1 Environmental Science Services Administration, Boulder, Colo. (J. Rinehart)
1 Geoexplor International Inc., Lafayette, Calif. (Dr. Giancarlo Facca)
2 Geothermal Kinetics Systems Corporation, Phoenix, Ariz.
  Ward H. Austin (1)
  Willis Burnside (1)

2 Getty Oil Company, Bakersfield, Calif.
E. L. Merrier (1)
M. Matjesic
1 Joseph I. O'Neill Co., Midland, Tex. (E. T. Anderson)
1 Lamar-Merrifield Company, Santa Monica, Calif. (Dr. Paul Merrifield)
2 Magma Power Company, Los Angeles, Calif.
B. C. McCabe (1)
Tad Travers (1)
1 Marine Mineral Technology Center, Tiburon, Calif. (M. J. Cruickshank)
1 Northwest Public Power Association, Vancouver, Wash. (Henry Curtis)
1 Ocean Resources, Inc., La Jolla, Calif. (John L. Mero)
1 Pacific Energy Corporation, Marina Del Rey, Calif. (Dr. R. W. Rex)
1 Pacific Gas & Electric Company, San Francisco, Calif. (Director of Planning)
1 Phillips Petroleum Company, Del Mar, Calif. (Geothermal Operations Manager, Fred Terry)
1 R. A. Rowan & Company, Los Angeles (George D. Rowan)
1 Regional Oil and Gas Supervisor, Los Angeles, Calif. (Donald W. Solanas)
1 Sacramento State College, Sacramento, Calif. (Department of Engineering, Howard L. Hartman)
1 Southern California Edison Company, Los Angeles, Calif. (Russ H. Robinson)
1 Standard Oil Company of California, San Francisco, Calif. (Robert Greider)
1 Stanford University, Stanford, Calif. (Department of Mineral Engineering)
1 Thermal Power Company, San Francisco, Calif. (Earl T. English)
1 Union Oil Company, Los Angeles, Calif. (Dr. C. Ott)
3 United Nations Resources and Transportation Division, New York, N. Y.
C. J. Bonwell (1)
James McNitt (1)
Tsvi Meidav (1)
2 University of Arizona, Tucson, Ariz.
W. C. Lacey (1)
Department of Geosciences, Jerome Wright (1)
3 University of California, Riverside, Calif. (Department of Geological Science)
Shawn Biehler (1)
Lewis Cohen (1)
James Combs (1)
1 University of California, Lawrence Radiation Laboratory, Livermore, Calif. (Dr. A. L. Austin)
1 University of Nevada, Reno, Nev. (Consulting Geologist, Dr. Edmond Lawrence)
4 University of Utah, Salt Lake City
Director, State Geological Survey (1)
W. Perry (1)
Robert B. Smith (1)
John E. Willson (1)
1 W. O. and J. I. Anderson, Los Angeles, Calif.